Arabian Journal of Geosciences (2021) 14: 906
https://doi.org/10.1007/s12517-021-07284-z

ORIGINAL PAPER

Petrology and geochemistry of pegmatites and associated rocks in Wamba areas, northcentral basement complex, Nigeria: implications for petrogenesis and rare-metal mineralizations

Anthony Chukwu[1] · Smart Chika Obiora[2]

Received: 27 January 2021 / Accepted: 7 May 2021 / Published online: 17 May 2021

Abstract

This study presents the field, petrography and geochemical data of the late Neoproterozoic pegmatites and host rocks in northcentral basement complex of Nigeria. Wamba pegmatites are emplaced within the reworked belt of the Nigerian basement complex. The pegmatites are composed of complex partly zoned (rare-metal pegmatites) and sparse simple (barren) pegmatites. They occur mostly as dyke (NE-SW) in migmatite-gneiss complex composed of mainly migmatitic gneisses and muscovite-biotite gneisses. The complex pegmatites are generally composed of albite, muscovite and quartz with accessory of garnet, tourmaline, beryl, ilmenite, apatite and cassiterite-columbite-tantalite minerals. The minerals show overlapping variations across the zones with albite-tourmaline wall zone, albite-beryl intermediate and quartz-spodumene core zone. The simple pegmatite constitutes of quartz, microcline and biotites. Muscovites and albite occur as minor components. The host rocks are composed of quartz, plagioclase, microcline, muscovite and biotite. Cordierite, garnet, sillimanite and hornblende are minor. The pegmatites and paragneisses are highly peraluminous with the complex pegmatites showing internal fractionation. The complex pegmatites exhibit low K/Rb, Nb/Ta and Mg/Li with relative enrichment in Rb, Li, Cs, Be, Sn, Nb and Ta from wall to core zone. The pegmatites and host rocks show similar geochemical signatures; equilibrium batch melting model further indicated crustal origin with the pegmatites as anatexis products of post-collisional reactivation of the high-grade metamorphic terrain. The rare elements formed by low-temperature partial melting of biotite-bearing pelitic rocks and contribution of hydrothermal fluids which led to albitization and metasomatism that result to high concentration of Sn.

Keywords Wamba · Complex pegmatites · Migmatitic gneiss · Peraluminous · Anatexis

Introduction

The origin and classifications of pegmatites has been major subject for debates among researchers for centuries. Jahns and Burnham (1969) argue in favour of fractional crystallization of a granitic pluton, while Simmons et al. (1995) believed that pegmatites originated by low-degree partial melting of crustal rocks in the presence of fluids. However, in some situations, these two processes can occur together with the former preceding the latter (Shaw et al. 2016). There are worldwide examples of rare-metal pegmatites generated by fractional crystallization of batholiths such as Yichun Hill, China; Indian Hill, southern California; and north Pilbara Craton, Western Australia among others, while the Fraser Lake area of Northern Saskatchewan, Canada; Munchberg Massif, Germany; and Mt. Mica pegmatites, ME, USA (Simmons et al. 2016) are few examples of pegmatites formed by direct partial melting.

The Wamba pegmatite fields (Jacobson and Webb 1946; Matheis 1987; Kuster 1990) located in northcentral Nigeria reworked Pan African belt which is one of the oldest pegmatite fields in Nigeria ("the old tin field"). Other fields are located in north, southwestern and southeastern basement complex of Nigeria typified by Egbe and Ijero pegmatite fields (Fig. 1)

Responsible Editor: Domenico M. Doronzo

✉ Anthony Chukwu
achukwu1@gmail.com; anthony.chukwu@ebsu.edu.ng

Smart Chika Obiora
smart.obiora@unn.edu.ng

[1] Department of Geology, Faculty of Science, Ebonyi State University, Abakaliki, Nigeria

[2] Department of Geology, Faculty of Physical Sciences, University of Nigeria, Nsukka, Enugu State, Nigeria

(Jacobson and Webb 1946; Okunlola 2005). The rare-metal pegmatites in Nigeria are dated from 560 to 450 Ma by Rb/Sr and U/Pb methods with Wamba area accounted for 537–522 Ma (Matheis and Caen-Vachette 1983; Matheis 1987; Melcher et al. 2015). The major host rocks of the pegmatites in northcentral basement is the migmatitic gneisses, while the southwestern pegmatites are confined to metavolcanosedimentary belts (Matheis 1987; Chukwu and Obiora 2021b). However, host rocks of schist and granodiorites are reported around Keffi areas, northcentral by Okunlola and Ocan (2009), Akintola and Adekeye (2008) and Akoh et al. (2015). The pegmatites in the Wamba area have recorded mining of rare metals by small-scale mining in rock outcrops, eluvial and alluvial placers. The Wamba pegmatites have close spatial relationship with the rare-metal (tin and columbite) mineralized Jurassic ring complex granites of Jos Plateau (about 60 km NW of Wamba), otherwise known as the younger tin fields of Nigeria, but the Jurassic granites are anorogenic (Kuster 1990) (Fig. 1). Jacobson and Webb (1946), Kuster (1990) and Akintola and Adekeye (2008) linked the pegmatites in northcentral Nigeria to the Pan-African granites (older granites) which are a suite of orogenic granitoids of upper Proterozoic-Palaeozoic age. The granites in most locations are several kilometres away from the pegmatites. Kuster (1990) arguement that the pegmatites crystallize from the granites are based on trace elements ratios without considering the migmatite gneisses which host the pegmatites in most locations. But also acknowledged that the exact granite-pegmatite relationship are very difficult to identify due to multiphase of the Pan-African activities and ability of individual plutons to release residual melts. However, recent geochronological data (560–450 Ma) presented by Melcher et al. (2015) put doubts on the genetic relationship between the pegmatites and the older granites. Furthermore, earlier work by Matheis (1987) and lately Chukwu and Obiora (2021b) suggested that the rare-metal pegmatites in the southwestern and northcentral Nigeria may be

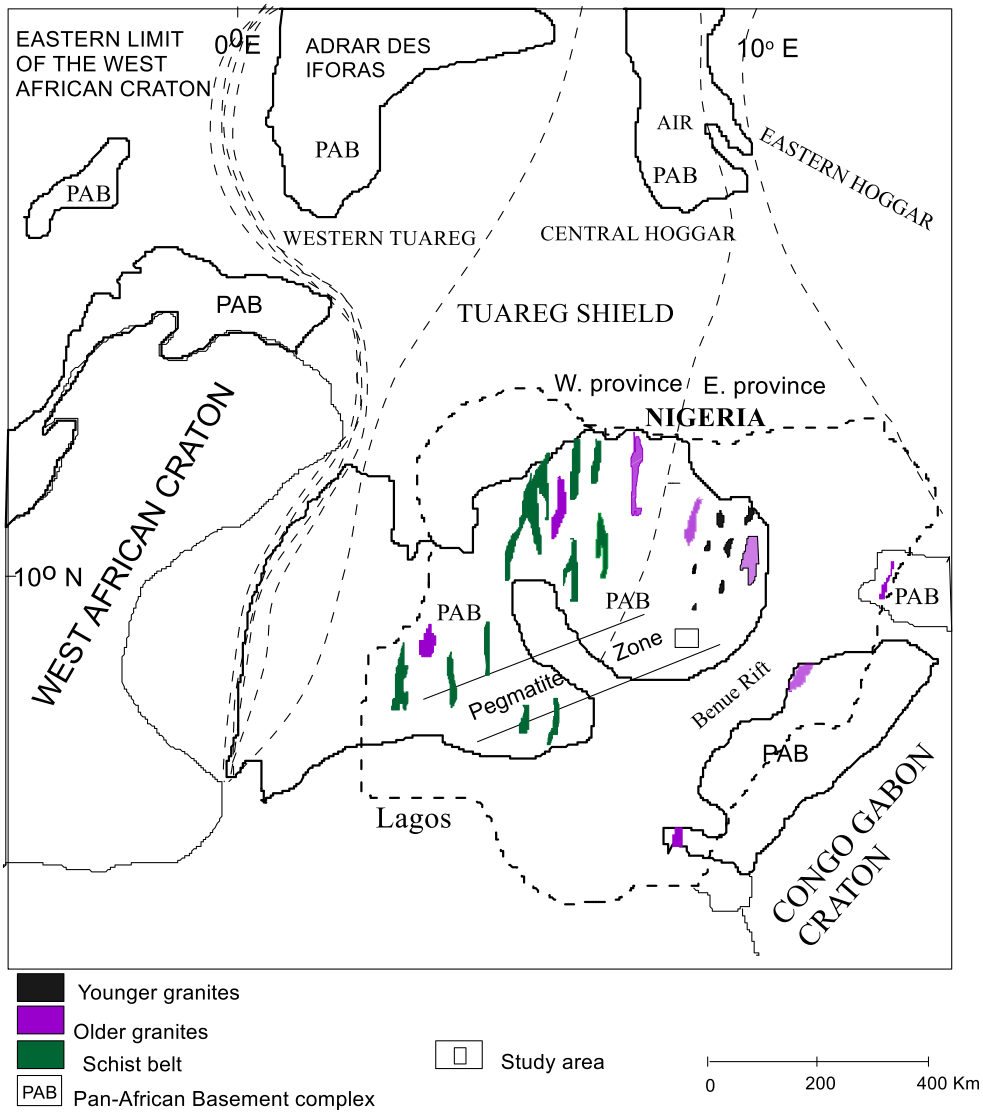

Fig. 1 Generalized map of Pan-African basement complex east of West African craton showing position of Nigeria and zone of pegmatites. Modified after Obiora and Ukaegbu (2009)

derived from the reactivation of tectonic fractures and partial melting.

The pegmatites in Wamba area have not been investigated for the past 3 decades, and previous works in the area are very sparse and even the few available ones focused mainly on the mineralization control. Jacobson and Webb (1946) and Kuster (1990) were of the opinion that the pegmatites originated from extended fractional crystallization of parent Pan-African granites, even where no major granitic intrusion is known. There are no comprehensive data on whole rock analysis of these pegmatites and host rocks with respect to their petrogenesis. This paper presents the detailed field distribution and characteristics of the pegmatites in Wamba area, mineralogical and whole rock analysis of the pegmatites and associated host rocks in order to infer their petrogenetic relationships especially in the light of the recent age discovery on the pegmatites.

Geological settings and local geology

Nigerian basement lies within the Upper Proterozoic to Lower Phanerozoic Pan-African reactivated mobile belt. It is located east of West African Craton and south of the Tuareg shield and extends from Algeria through southern Sahara, Nigeria, Benin and the Cameroons (Fig. 1). The reactivated mobile belt extends beyond Africa to northeastern Brazil where comparable rare-metal pegmatites are also mapped (Jacobs and Thomas 2004). The Pan-African mobile belt is believed to be generated through collision of the active continental margin of the Pharusian belt and the passive continental margin of the West African Craton about 600 Ma (Burke and Dewey 1972). Subduction and subsequent collision at the eastern margin of the West African Craton closes the ocean and extensive melting of the older rocks resulted in the emplacement of the mostly calc-alkline granitoids and basaltic intrusions (McCurry and Wright 1977).

The Nigerian Basement rocks have undergone series of orogenic cycles that are characterized by deformation, metamorphism, reactivation and remobilization which results to extensive migmatization. This corresponds to the Liberian (2650 ± 150 Ma), the Eburnean (2000 ± 50 Ma) and the Pan-African cycle (600 ± 150 Ma). In addition, Grant et al. (1972) and Odeyemi (1981) also reported Kibaran (1100 ± 200 Ma) rocks around southwestern and northcentral Nigeria. Three lithologic units have been recognized (Fig. 1): the migmatitic gneiss complex which comprises biotite and biotite hornblende gneisses, quartzites and quartz schist and small lenses of calc-silicate rocks; slightly migmatized to unmigmatized paraschists and metaigneous rocks which comprise pelitic schists, quartzites, amphibolites, talclose rocks metaconglomerates, marbles, banded iron-formations and calc-silicate rocks; and older granites which comprise granodiorites, granites and potassic syenites. The migmatitic gneiss represents the oldest sequence of the basement complex followed by the schist belts and metaigneous rocks and intruded by the Pan-African granites (older granite). The metamorphism of the migmatitic gneiss complex is in amphibolite to granulite facies grade; the schist belt which is essentially N-S to NNE-SSW trending belts and concentrated more in western half of the Nigeria is greenschist-amphibolite facies (Ajibade and Wright 1989). The rocks of the schist belt host the gold and rare-metal mineralization pegmatites mostly in southwestern Nigeria. The Pan-African granites which are syn-post-collisional plutons are found all the parts of the basement complex. The Pan-African granites in the central and southeastern basement complex of Nigeria are subdivided into two groups. The earlier group is approximately 640–600 Ma suites of peraluminous biotite-muscovite granites and the latter is approximately 600–580 Ma suite of trans-alkaline hornblende-biotite granitoids (Ferré et al. 2002). The Pan-African granites in the southwestern basement complex (Fig. 1) are hornblende-biotite granites and were considered to be I-type granitoids and dated 630–580 Ma similar to those of the central and southeastern Nigeria (Goodenough et al. 2014). The Mesozoic alkaline plutons (younger granite) that are known for tin and niobium production are restricted in the northcentral basement complex close to Jos plateau. Similar Neoproterozoic plutons are also mapped in Ghana, Togo and Benin (c. 660–550 Ma) and Borborema Brazil (c. 630–610 Ma). Late Jurassic-Cretaceous intrusive and extrusive igneous rocks are known to occur in Nigerian sedimentary basins within the NE-SW trending Nigerian Benue rift (Chukwu and Obiora 2014, 2018, 2021a; Fig. 1).

The post-collisional magmatism in Nigeria is associated with rare-metal granitic pegmatites (Matheis and Caen-Vachette 1983; Kuster 1990; Okunlola 2005; Goodenough et al. 2014). The pegmatites dated 560–450 Ma (Matheis and Caen-Vachette 1983; Melcher et al. 2015) are quite younger than the Pan-African granites, and the age gap opened a new point of discussion on the origin of the pegmatite earlier believed to be associated with the Pan-African granite.

The study area Wamba and surroundings are underlain by the reactivated basement complex of the northcentral Nigeria. The area is highly migmatized and characterized by rocks of metamorphic grade of amphibolite to granulite facies in most locations. The dominant rock types in the area are the migmatitic gneiss and muscovite-biotite gneiss (Fig. 2). They are intruded by the minor leucogranites, doleritic rocks and mineralized granitic pegmatites (Fig. 2).

Migmatitic gneiss

The migmatitic gneiss occupies more than 70% of the study area and represents the host of other rock units in the area. It consists of minor subunits of biotite-gneiss, augen gneiss and banded gneiss. They outcropped as large hills which extend as ridges, while others occur as low-lying ridges at the base of river channels in the area such as the Shariga River. The hilly

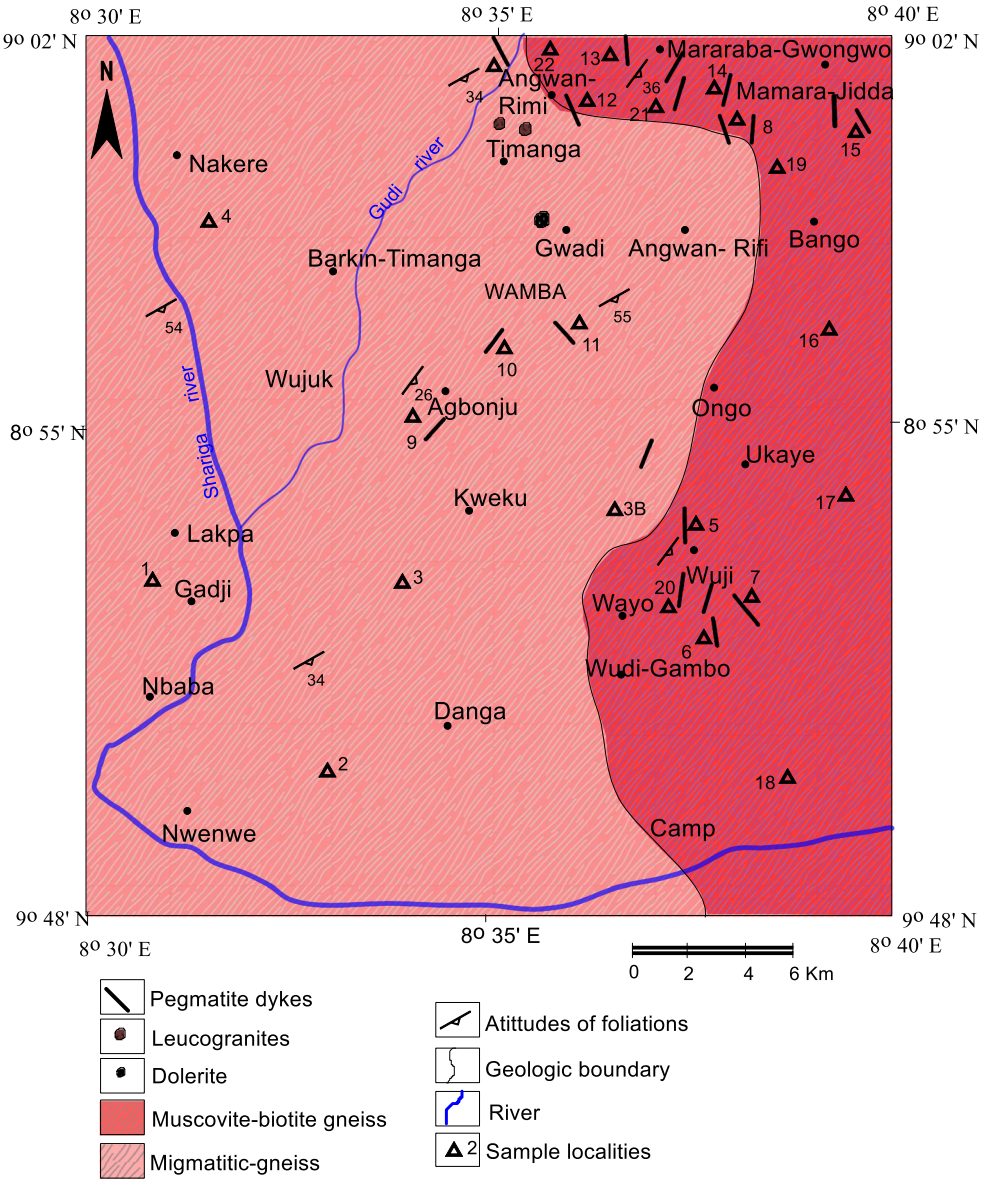

Fig. 2 Geological map of Wamba area indicating locations of the pegmatites in relation to the host rocks

outcrops are oval shaped, more than 130 m high and continue intermittently in NE-SW orientations over kilometres with sharp valleys in-between. The intensity of metamorphism in the migmatitic gneiss outcrops can be seen in the banding of the gneissose foliations (Fig. 3a) and other complex structures showing evidences of deformations. The banding shows segregations between the light and dark components and augen structures characterized by orthoclase and andesine, giving the rock a porphyroblastic texture. The migmatitic gneiss is composed of the leucosome, mesosome and melanosome components. The leucosome are granitic in composition, light coloured, coarse grained and consists of alignment of platy mineral (mica). The major mineralogical components are quartz, potassium feldspar and plagioclase (andesine), biotite and muscovite. The melanosome is melanocratic, medium to coarse grained and possess schistose foliations. They represent the restite of the older rocks (Fig. 3b) that mostly probably resisted partial melting. This formed pinch and swell structures that also show intense plastic deformation of the terrain. The mineral components of the melanosome are mainly quartz, plagioclase, biotite and hornblende. Cordierite and magnetite occur as accessory. Biotite is the major mafic component. The mesosome is coarse grained and the mesocratic portion of the rocks. The foliations trend in NNE-SSW with average dipping plane of about 35°. The foliations are banded and folded in contour-like structures (Fig. 3a) which are obvious in the Shariga River to Agbonju hill outcrops. Other structures that occur in this migmatites unit are granitic in compositions such as quartzo-feldspathic veins and veinlets of about 0.5 to 6 cm, dominantly concordant to the foliation planes, while others cross-cut the foliations. Ptygmatic folds and lit-per-lit injections are common especially in Agbonju

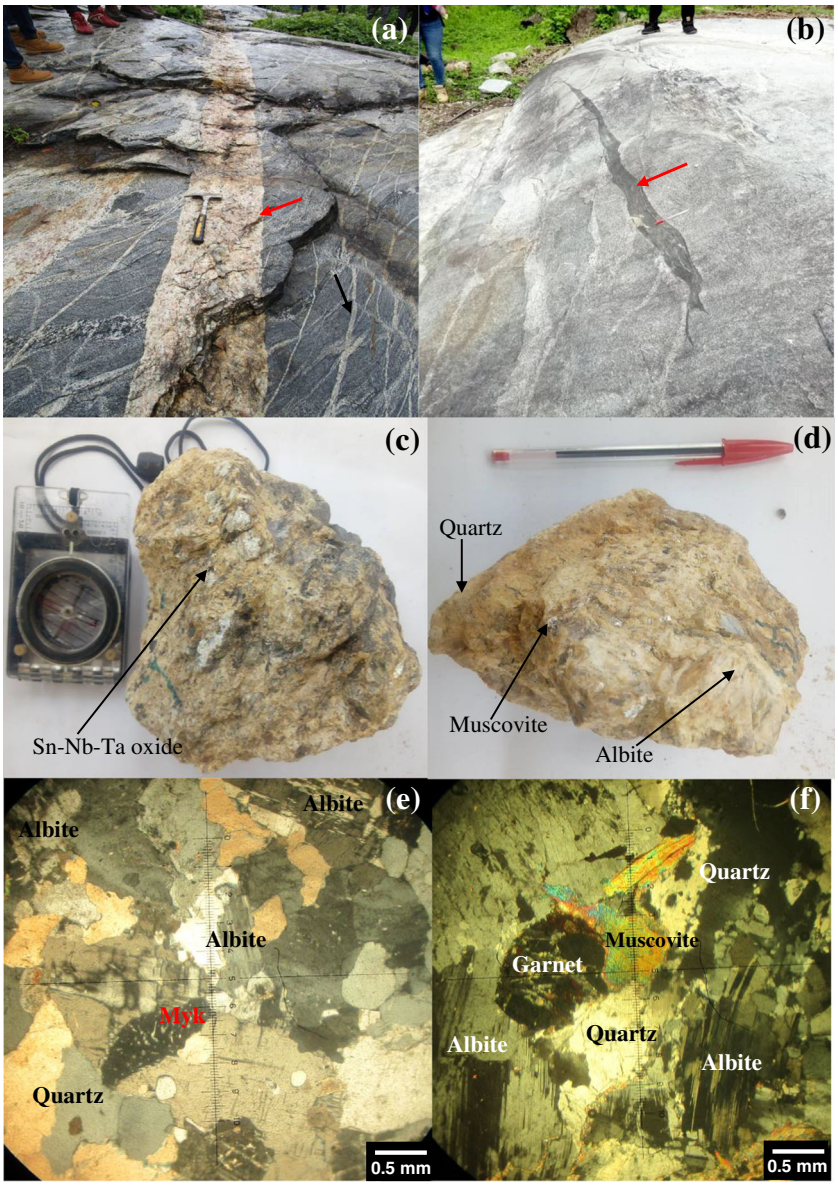

Fig. 3 **a** Exposure of the coarse grained migmatitic banded gneiss at Agbonju hill, cross-cut by biotite-microcline-quartz pegmatites (red arrow) and several quartzo-feldspathic veins (black arrow); **b** mesocratic components of the migmatitic gneisses showing lensoidal like relict of resisted older metasediment (red arrow) during high-grade metamorphism; **c** and **d** show intermediate and core zones respectively of the complex pegmatites from Mararaba Gwongwon artisanal mines; **e** photomicrograph in cross-polars of the complex pegmatite showing quartz graphically intergrown with albite (myk= myrmekite); **f** complex pegmatites showing crystals of albite, quartz and muscovite closely associated with embayed garnet

hill location (central part of the map). Meta-basic and granitic pegmatite dykes with thicknesses ranging from 1 to 4 cm and 2 to 40 cm, respectively, transverse the outcrops and obvious at Agbonju hill location (Fig. 3a). There are several deformations (dextral and sinistral strike-slip faults) across the foliations, granitic dykes and basic dykes around the outcrops. These structures and dislocations attest the episodes of the Pan-African polycyclic dislocations and show high-grade metamorphism and anatexis.

Muscovite-biotite gneiss

This rock type occurred mainly towards the eastern parts of the map area (Fig. 2). They are the predominant host of the complex (rare-metal) pegmatites. The rocks are leucocratic to mesocratic, coarse grained and possess gneissose foliations in NNE-SSW orientation. They also show deformations such as folding of foliations, strike-slip faults and evidences of partial melting such as ptygmatic folds. Mineral compositions are similar to granitic rocks such as quartz, plagioclase, k-feldspar, muscovite and minor biotite. Accessory minerals include garnet, cordierite, ilmenite and zircon. The muscovite-biotite gneiss observed in Gwongwon area has gradational contact with the complex pegmatites. They are possibly slightly metasomatized by hydrothermal fluids resulting from the emplacement of the pegmatites.

Pegmatites

The pegmatites are abundant in the muscovite-biotite gneiss and the migmatitic gneiss in the Wamba area than other rock types in the area. More than 27 cross-cutting dykes were

mapped within the study area. The pegmatites are generally low lying, and thickness varies from 60 cm to 4 m and extensively more than 25 m wide in some locations while the length is beyond 50 m. Some dykes continue with disruption to more than 1 km. They have sharp contacts with the host rocks in most locations, but few bodies show gradational contact (due to minor metasomatic interaction with muscovite-biotite gneiss) at the boundary with the host rock around Gwongwon area of Wamba. The pegmatites are very coarse grained, light coloured and possess graphic texture (Fig. 3 c and d). The pegmatites mostly trend NNE-SSW and NW-SE directions with few trending NNW-SSE. The dip of the pegmatites is mainly vertical, but some varies according to the depth of accommodating fractures, which shows that the pegmatites were emplaced following existing fractures in the migmatitic rocks. This support the suggestion by Matheis (1987) that the pegmatites in Nigeria are structurally controlled. Based on field and mineralogical compositions, the pegmatites are divided into simple massive pegmatites and complex (partly zoned) tabular pegmatites. The simple massive pegmatites occurred mostly within the migmatitic gneiss, around the Agbonju hills, Wamba gate and Mechanic site (Fig. 2), and trended mainly in NE-SW directions, while the complex partly zoned pegmatites (rare metal) occurred mostly within the muscovite-biotite gneiss which is abundant in the eastern part of the study area (Fig. 2). The complex pegmatites trend dominantly in NNE-SSW and NW-SE directions and sometimes occur within weathered profiles. Inferred zones in the complex pegmatites are thin wall zones (albite zone), broad intermediate zone (beryl zone) and quartz core zone. The complex pegmatites (rare metal) are prominent in notable localities in the study area such as the Angwa-Rimi pegmatite, Maramara pegmatite, Mararaba-Gwongwon pegmatite and Wuji pegmatite (see Fig. 2). Based on the mineralogical compositions, the simple pegmatites can be known as biotite-microline-quartz pegmatites while the complex pegmatites as albite-muscovite-quartz pegmatites.

Petrography

Migmatitic gneiss

The minerals in the migmatitic gneiss are generally quartz, potassium feldspar and plagioclase (dominantly andesine) and biotite. Other minor and accessary minerals include hornblende, cordierite, sillimanite, muscovite, ilmenite and garnet. The migmatitic gneiss consists of thin layers of melanocratic portion dominated by brownish biotite and plagioclase (andesine-labradorite). Other minor constituents are hornblende, sillimanite and orthopyroxene alternating with leucocratic layer that consists of quartz, microcline and plagioclase (oligoclase-andesine) and minor garnet and cordierite. The presence of garnet and cordierite suggests a sedimentary origin. The quartz is milky coloured, subhedral to anhedral and exhibits undulatory extinction which shows deformation. Common K-feldspar is microcline that is characterized by pinkish to colourless and polysynthetic twinning. The microcline has inclusions of quartz and biotite in some locations. Plagioclase constitutes more than 40% of the mineral composition in migmatitic gneiss. They are colourless, prismatic and show cleavage in one direction and albite twinning. Andesine and less sodium rich constitute more of the light coloured components, while andesine and labradorite constitute the dark components. Myrmekite form boundary between plagioclase and quartz. Biotite and hornblende constitute the mafic components. Garnet occurs as fractured fragments and associated with muscovites with inclusions of plagioclase. Mineralogical composition also suggests pelitic protolith. The assemblage of garnet – sillimanite – orthopyroxene ± cordierite suggest high temperature and pressure metamorphism between high amphibolite to granulite facies with temperature above 800° C (Ferré et al. 2002) that leads to anatexis.

Muscovite-biotite gneiss

The muscovite-biotite gneiss composes of quartz, plagioclase, k-feldspar, muscovite and biotite. Sillimanite also occurs as minor constituent. Accessory minerals include garnet, cordierite, ilmenite and zircon. Quartz is colourless, anhedral, prismatic and also undergoes undulatory extinction similar to the migmatitic gneiss. Plagioclase (andesine) is the dominant mineral (more than 55%) in the rock and secondary albite and muscovites which are fine grained, formed by replacing orthoclase and biotite through albitization and muscovitazation, respectively. Biotite and hornblende constitute the mafic component. The muscovite is colourless to pale green, showing bent cleavages which support microdeformation. Garnet and aggregate of tourmaline occur mostly as inclusion at the contact with the pegmatites suggesting metasomatism of the host rock. Microcline occurs as subhedral and show polysynthetic twinning (cross-hatch).

Pegmatite

The simple pegmatites contain smoky quartz, brown biotite and pinkish microcline as major constituents. Albite, garnet, magnetite, white muscovite and black tourmaline (schorl) occur as accessory minerals. The complex pegmatites are partly zoned into wall zone, intermediate zone and core zone. The wall zone (albite zone) has medium grained of albite, white to pale green muscovite, white to pinkish microcline, and quartz. Garnet and black striated tourmaline are dominant accessories; others are apatite, cassiterite and niobium-tantalite oxide. Intermediate zone is broader than other zones, very coarse grained and consists of albite (cleavendite), pinkish

microcline-perthite, pale greenish muscovite, quartz and beryl. Accessories are embayed garnet, cassiterite and niobium-tantalite oxide. The quartz core zone is rich in milky quartz, albite (cleavendite), muscovite and occasional spodumene. Garnet, cassiterite and niobium-tantalite oxides constitute the accessory phase. Alteration in the pegmatites is more of albitization where microcline is replaced by albite and breakdown of biotite to chlorite.

Quartz crystals are colourless to milky, anhedral towards the wall zone and subhedral to euhedral in the core zone. Albite is the most common mineral in the pegmatites with large crystal up to 5–10 cm in some cases, it is colourless, prismatic and with cleavages in two directions (basal section) and pronounce albite twinning according to albite law with low extinction angles. Graphical intergrowth between quartz and albite (myrmekite) is common in the wall zones (Fig. 3e). Large albite crystal contains inclusions of aggregates of muscovite, garnet and tourmaline crystal (Fig. 3f). Microcline and perthite are pinkish, colourless in thin section. It is prismatic, subhedral to euhedral towards the core zone and cleavages in longitudinal section. Cross-hatching twinning is common in the microcline. Biotite occurs in most of the rocks including the pegmatites except the zoned pegmatites. It is dark and brownish in sections, thin cleavages in one direction, flaky and exhibits parallel extinction in most sections. The primary biotites are large flakes 3–7 cm diameter, while the secondary biotite occurs combined with the primary biotite in the simple pegmatites and easily altered to chlorite. Muscovite occurs in all the zones but dominant in the intermediate zone and as accessory in the simple pegmatites. They are pale green to transparent, silver-coloured in simple pegmatites. The crystals are euhedral (up to 10 cm) and possess cleavages in one direction with parallel extinction. Garnet in the pegmatites occurs as euhedral to subhedral embayed crystals with inclusions of tiny quartz, plagioclase and muscovite. They form as a product of biotite-dehydration melting reaction followed by textural modification.

Analytical procedure

A total of twenty-two samples of the pegmatites about 4–5 kg to represent average grain size of the coarse grained rocks and associated host rocks were collected. The migmatitic gneisses, muscovite-biotite gneisses and simple pegmatites were sampled appropriately. Thereafter, the fine-medium grain wall zone, 4–5 kg large samples of the intermediate and core zones of the partially zoned pegmatites were sampled to represent average composition of each zone. The samples were pulverized by tungsten mill at the Laboratory of Department of Geology, University of Nigeria, Nsukka, homogenized and 100 g each and sent to Genalysis (Intertek) Laboratory Services Pty Ltd, Maddington, Australia for analysis. The major oxides were analysed by X-ray fluorescence (XRF) with duplicate samples better than 1%. The trace elements were analysed using inductively coupled plasma mass spectrometry (ICP-MS) after a fusion of the sample with lithium metaborate/tetraborate. However, B and Li were determined using ICP-MS after a fusion of the sample with sodium peroxide. Loss on ignition (LOI) was determined by robotic thermogravimetric analyser (TGA). Detection limits is 0.01 wt% for major oxides; 5 ppm for Li, Nb and Zr; 2 ppm for Sn; 0.1 ppm for Ta, Cs, Hf, Th and U; 0.5 ppm for Rb, Pb, Ce and Y; and 1 ppm for Ba, Ga and W. Blanks and duplicate were analysed to ensure quality control of each analytical techniques. Certified standards used for accuracy are AMIS0340, OREAS 45d, OREAS 24b and SARM1.

Results

Geochemistry

Migmatitic gneiss

The major oxides are presented in Table 1. The migmatitic gneisses SiO_2 values range from 60.75 to 66.62 wt%. The values of TiO_2, Fe_2O_{3tot}, MnO, MgO, CaO and P_2O_5 are relatively high. The values of Al_2O_3, Na_2O and K_2O across the rock samples are generally high, with Al_2O_3 having the highest concentrations ranging from 14.47 to 17.34 wt%. Generally, $K_2O > Na_2O$ across the host rocks and NaO+ K_2O values range from 6.33 to 9.35 wt%. Loss on ignition (LOI) values across the host rocks are generally low (< 0.6 wt%) in the unit. The migmatitic gneiss rock samples are strongly peraluminous with alumina saturation index (ASI) ranging from 1.04 to 1.62.

The average concentrations of Ba and Sr are higher (Ba, 948 ppm and Sr, 360 ppm) compared to average crustal abundances (Ba, 584 ppm and Sr, 333 ppm) of Wedepohl (1995). The average values of Rb, Li, Sn, Cs, Be, W and Ga vary across the rock samples and higher than the average crustal abundance, while Nb and Ta values are lower than the average crustal abundances. The host rocks are generally depleted in Co, Cr, Cu, Ni and Mo transitional metals compared to average crustal abundances of 24 ppm, 126 ppm, 25 ppm, 56 ppm and 1.1 ppm, respectively, of Wedepohl (1995), while Pb, Zn and Zr are relatively higher than their corresponding average crustal abundances.

Muscovite-biotite gneiss

The muscovite-biotites gneisses are the most evolved with highest silica contents (SiO_2 > 70 wt%) except sample (CA22) which has low SiO_2 54.58 wt% (Table 1). This sample (CA22) of the muscovite-biotite gneiss has close contact

Table 1 Major element oxides (wt%) and trace element (ppm) composition of the pegmatites and host rocks from Wamba area

	Migmatitic gneiss				Muscovite-biotite gneiss				MMG	Simple pegmatite			Complex pegmatites (wall zone)		Complex pegmatites (interm. Zone)				Complex pegmatites (core zone)			
	CA1	CA2	CA3	CA4	CA16	CA17	CA18	CA19	CA22	CA9	CA10	CA11	CA5	CA6	CA7	CA8	CA12	CA13	CA14	CA15	CA20	CA21
SiO_2	66.62	60.75	61.73	63.26	71.19	74.15	73.86	71.43	54.58	73.41	72.13	75.03	76.09	71.64	74.93	76.05	71.99	64.12	71.69	72.14	74.69	72.43
TiO_2	0.69	0.85	0.53	0.71	0.36	0.26	0.12	0.43	1.17	0.01	0.01	0.07	0.01	0.01	0.02	0.01	0.01	0.01	0.02	0.01	0.01	0.01
Al_2O_3	14.75	17.01	14.47	17.34	14.82	13.68	14.25	14.97	21.73	15.01	15.42	13.97	14.89	16.77	14.15	13.59	15.9	18.27	14.76	15.01	14.15	15.68
Fe_2O_3	4.36	6.25	4.84	5.36	2.5	1.54	1.01	2.21	6.72	0.91	0.53	0.66	0.98	0.62	1.62	1.41	0.66	1.13	0.9	1.1	1.57	1.08
MnO	0.11	0.11	0.15	0.1	0.07	0.05	0.03	0.04	0.18	0.21	0.13	0.03	0.14	0.04	0.37	0.25	0.05	0.16	0.09	0.16	0.13	0.12
MgO	0.63	2.64	3.71	1.97	1.26	0.33	0.36	0.55	2.01	0.04	0.03	0.08	0.11	0.04	0.06	0.05	0.03	0.03	0.06	0.03	0.08	0.05
CaO	2.88	4.71	6	4.45	2.19	1.06	1.09	2.04	2.95	0.1	0.15	0.78	0.07	0.36	0.27	0.4	0.34	0.37	0.26	0.41	0.52	0.29
Na_2O	2.98	4.29	3.28	4.26	3.4	3.41	3.41	4.27	4.64	3.14	2.76	3.18	4.01	8.91	3.29	4.13	5.85	3.09	2.35	5.15	2.77	5.65
K_2O	6.37	2.69	4.67	2.07	3.93	5.24	5.61	3.73	2.83	6.55	8.19	5.9	2.52	0.84	3.36	2.6	4.6	11.01	8.94	4.03	3.42	3.49
P_2O_5	0.213	0.298	0.136	0.29	0.102	0.072	0.04	0.104	0.59	0.181	0.27	0.024	0.117	0.412	0.55	0.604	0.398	1.171	0.665	0.79	0.746	0.537
LOI	0.36	0.5	0.47	0.57	0.39	0.28	0.36	0.33	2.18	0.47	0.39	0.26	1.12	0.27	1	0.86	0.22	0.46	0.42	0.53	1.43	0.69
Total	100.26	100.38	100.29	100.6	100.36	100.19	100.26	100.28	100.18	100.1	100.07	100.11	100.12	99.96	99.7	100.04	100.11	99.93	100.3	99.45	99.62	100.13
Na_2O+K_2O	9.35	6.98	7.95	6.33	7.33	8.65	9.02	8	7.47	9.69	10.95	9.08	6.53	9.75	6.65	6.73	10.45	14.1	11.29	9.18	6.19	9.14
ASI	1.20	1.45	1.03	1.60	1.55	1.40	1.40	1.49	2.08	1.53	1.38	1.41	2.25	1.65	2.04	1.90	1.47	1.26	1.27	1.56	2.11	1.66
A/NK	1.574	2.43	1.82	2.73	2.02	1.58	1.57	1.87	2.90	1.54	1.40	1.53	2.28	1.72	2.13	2.02	1.52	1.3	1.31	1.64	2.29	1.72
Trace elements																						
Li	41	62	27	68	57	88	11	66	628	15	32	9	44	21	114	68	20	38	80	30	161	40
B	23	67	30	23	X	32	27	X	X	X	44	X	49	bdl	78	91	40	28	bdl	bdl	21	bdl
Ba	1507	717	1153	415	444	230	371	624	2544	24	28	376	26	24	19	59	68	186	501	278	171	189
Be	2.41	4.19	15.92	4.49	10.36	4.26	3.82	5.02	20.61	5.04	4.87	3.98	7.56	156.32	75.83	282.25	165.21	527.88	5.98	7.7	9.14	8.7
Bi	0.06	0.09	0.08	0.05	0.21	0.11	0.19	0.07	0.08	3.69	0.13	0.18	8.8	0.13	19.32	0.26	0.17	0.11	0.24	0.05	0.03	0.05
Ce	56	68	51.7	54.4	59.5	67.2	15	47.5	149.6	3.1	1.3	53.8	2.9	1.1	0.6	0.5	0.6	8.3	19.5	4.1	1.6	21.9
Co	14.3	23	17.6	15.5	13.3	13	15.8	10.7	15.9	9.9	19.5	9.4	5.9	3.7	4.3	8.3	7.6	9.9	5.3	8	28.8	13.5
Cr	2	23	31	9	36	4	12	4	7	2	2	2	bdl	bdl	1	2	bdl	1	2	1	2	bdl
Cs	2	8.2	9	5.3	21.1	9.2	3	15.9	83.5	9.3	12.1	2.8	10.4	6.7	16.1	14.1	21.8	32.8	21.9	12.9	23.6	9.5
Cu	2.4	9.7	4.1	30.2	5.9	8.5	12.3	2.4	9.3	1.6	3.5	15.4	2.3	2.4	6.6	8.8	3.9	26.3	2.9	0.8	1.6	1.1
Ga	19	23	18	23	20	18	17	27	30	24	26	19	46	47	53	51	35	44	28	35	54	34
Hf	6.8	5.2	7.1	3.5	3.4	5.6	2.4	4.1	20.1	2	0.6	2.6	4.7	1.7	0.4	0.3	1.4	0.4	5.5	2.5	1.7	1.3
Mo	0.8	0.4	0.5	0.4	0.2	0.3	0.7	0.2	X	0.2	0.3	0.8	0.1	bdl	0.1	0.2	0.2	0.3	0.6	0.1	0.2	0.3
Nb	8	10	10	12	9	12	12	11	13	9	9	8	28	62	51	52	76	62	24	46	106	27
Ni	1.5	14.7	21.7	9.1	22.1	1.7	2.4	2.9	4.8	2	1.3	2.6	bdl	0.6	1.7	3.3	0.9	4.2	3.8	0.8	1.7	0.6
Pb	8.2	20.2	15.3	14.9	28.8	29.1	37.2	32.5	17	16.4	14.6	37.7	5	2.8	3.7	2	11.5	21.7	20.6	3.1	1.4	9.4
Rb	152.8	118.1	115.7	94.8	196.9	146.7	143.2	204	754.9	405.5	559.8	147.7	329.5	146.7	599.8	464.8	818.7	1719.9	992.9	543.3	702.9	335.1
Sb	0.12	X	0.11	0.08	X	0.05	X	0.05	X	0.05	0.06	X	bdl	bdl	bdl	bdl	0.05	bdl	0.06	bdl	bdl	bdl
Sn	3	4	21	2	5	6	X	5	116	16	16	X	54	101	96	77	2059	274	23	3379	4466	740
Sr	189	593	241	419	164	89	151	261	624	X	X	141	26	37	32	40	37	82	116	100	172	74
Ta	0.8	0.9	0.9	1	1.5	0.7	0.6	0.9	1.1	0.9	1	0.4	2.3	18.7	4.3	4.9	42.6	21.7	4.3	23.8	45.3	6.2
Th	5.7	5.9	5.8	6.8	13.3	11.9	5.4	9.2	9.6	1.8	0.6	5.6	2.6	0.2	0.8	0.5	0.2	0.3	6.9	0.4	0.1	0.7
Tl	0.54	0.68	0.56	0.56	1.05	0.75	0.66	1.22	5.4	2.43	3.22	0.75	1.43	0.78	2.95	2.17	4.91	11.04	6.34	3.06	3.32	1.76
U	1.6	1.3	1.9	1.3	1.5	1.2	2.2	2.2	4.7	4	16.6	2.2	5.7	4.6	18.4	7.5	1.8	3.9	12.8	9.3	4	9.3
W	190	49	94	50	89	181	222	89	14	59	257	63	60	25	47	114	55	113	59	66	162	63
Y	54.4	19.8	44.3	25.7	8.7	10.5	6.7	6.1	17.5	6	2.9	5.7	3.7	1.3	0.4	0.4	2.2	5.9	4.6	7.4	1.1	6
Zn	43	91	66	81	49	38	16	75	176	17	15	13	30	41	111	123	30	42	71	65	104	46
Zr	250	192	308	129	119	157	64	129	997	35	13	61	83	17	6	7	11	9	110	28	15	17
Rare earth elements																						
La	25.4	30.6	19.5	24.5	29.8	36.8	10.4	24	76.5	1.3	0.7	18.6	1.1	0.4	0.3	0.3	0.5	11.8	11.5	2.5	0.3	11.3
Ce	56	68	51.7	54.4	59.5	67.2	15	47.5	149.6	3.1	1.3	53.8	2.9	1.1	0.6	0.5	0.6	8.3	19.5	4.1	1.6	21.9
Pr	7.4	8.2	6.6	6.7	6.5	6.3	1.9	5	16.5	0.4	0.2	3.8	0.4	0.1	0.1	bdl	0.1	2.9	2.3	0.7	0.2	2.8
Nd	34	33.5	30.2	27.3	23.8	21.3	6.9	19.1	67.7	1.3	0.8	12.1	1.3	0.2	0.3	0.5	0.6	10.1	8.6	3.8	1	11.7
Sm	8.7	6	7.5	6.1	4.3	3.1	1.2	3.3	9.5	0.7	0.3	1.9	0.9	0.2	0.2	0.2	0.2	1.9	2.2	0.8	0.3	2.2

Table 1 (continued)

	Migmatitic gneiss				Muscovite-biotite gneiss				MMG	Simple pegmatite			Complex pegmatites (wall zone)		Complex pegmatites (interm. Zone)			Complex pegmatites (core zone)			
	CA1	CA2	CA3	CA4	CA16	CA17	CA18	CA19	CA22	CA9	CA10	CA11	CA5	CA6	CA7	CA8	CA12	CA13	CA14	CA15	CA20	CA21
Eu	2	1.4	1.3	1.5	0.7	0.3	0.5	0.8	3.2	X	X	0.5	bdl	bdl	bdl	bdl	bdl	0.5	0.1	0.3	bdl	0.5
Gd	8.7	4.6	7.2	5.2	2.8	2.2	1.1	2.1	6.7	0.7	0.4	1.5	0.7	0.2	0.2	0.1	0.3	1.9	1.8	1	0.2	1.7
Tb	1.5	0.6	1.2	0.8	0.4	0.3	0.2	0.3	0.8	0.2	X	0.2	0.2	bdl	bdl	bdl	bdl	0.3	0.3	0.1	bdl	0.3
Dy	10.1	4	8.2	4.7	1.9	1.9	1.2	1.3	4.2	1.2	0.5	1	0.7	0.3	bdl	0.2	0.4	1.7	1.5	0.8	0.2	1.6
Ho	2	0.7	1.5	0.9	0.3	0.3	0.2	0.2	0.7	0.2	X	0.2	0.1	bdl	bdl	bdl	bdl	0.3	0.2	0.2	bdl	0.2
Er	6.2	1.9	5	2.6	0.8	1.1	0.6	0.5	1.9	0.4	0.2	0.5	0.3	bdl	bdl	bdl	0.2	0.7	0.3	0.5	bdl	0.6
Tm	0.9	0.3	0.7	0.4	0.1	0.1	0.1	X	0.2	0.1	X	X	bdl	bdl	bdl	bdl	bdl	bdl	bdl	bdl	bdl	bdl
Yb	6.1	1.9	4.5	2.3	0.7	1	0.6	0.5	1.7	0.7	0.2	0.5	0.3	0.1	0.1	0.1	0.2	0.5	1	0.5	0.1	0.5
Lu	0.9	0.3	0.7	0.4	0.1	0.2	0.1	X	0.2	X	X	0.1	bdl	bdl	bdl	bdl	bdl	bdl	bdl	bdl	bdl	bdl
∑REE	169.9	162	145.8	137.8	131.7	142.1	40	104.6	339.4	10.3	4.6	94.7	8.9	2.5	1.7	1.8	3.1	40.9	49.3	15.3	3.8	55.3
∑LREE	131.5	146.3	115.5	119	123.9	134.7	35.4	98.9	319.8	6.8	3.3	90.2	6.6	2	1.5	1.5	2	35	44.1	11.9	3.4	49.9
∑HREE	36.4	14.3	29	17.3	7.1	7.1	4.1	4.9	16.4	3.5	1.3	4	2.3	0.5	0.2	0.3	1.1	5.4	5.1	3.1	0.4	4.9
La/YbN	2.83	10.94	2.94	7.24	28.92	25.00	11.77	32.61	30.57	1.26	2.38	25.27	2.49	bdl	bdl	bdl	1.70	16.03	7.81	3.40	bdl	15.35
Eu/Eu*	0.70	0.81	0.54	0.81	0.61	0.35	1.33	0.93	1.22			0.90	bdl	bdl	bdl	bdl	bdl	0.80	0.15	1.02	bdl	0.79

MMG metasomatized muscovite-biotite gneiss, *Bdl* below detection limit

with the pegmatites and most probably undergone contact metasomatism. The values of TiO_2, Fe_2O_{3tot}, MnO, MgO, CaO and P_2O_5 are relatively lower compared to the migmatitic gneisses except in sample CA22, the metasomatized muscovite-biotite gneiss (Table 1). Similar to the migmatitic gneiss, the values of Al_2O_3, Na_2O and K_2O across the rock samples are also high, with Al_2O_3 also having the highest value of 21.73 wt% in the metasomatized muscovite-biotite gneiss. Generally, $K_2O > Na_2O$ and $NaO+K_2O$ values range from 7.33 – 9.02 wt% in the muscovite-biotite gneiss. Similar to the migmatitic gneisses, loss on ignition (LOI) values are very low (0.28–0.39 wt%) except the metasomatized muscovite-biotite gneiss (sample CA22) which has LOI 2.18 wt% indicating mild alteration by possibly hydrothermal fluids from the pegmatite melt. The muscovite-biotite gneiss rock samples are also strongly peraluminous with ASI values ranging from 1.41 to 1.56, while the metasomatized muscovite-biotite gneisses have the highest value of 2.09.

The average concentrations of Ba and Sr in the muscovite-biotite gneisses (Ba, 417.3 ppm and Sr, 166.3 ppm) are lower compared to average crustal abundances (Ba, 584 ppm and Sr, 333 ppm) of Wedepohl (1995) except the metasomatized muscovite-biotite gneiss sample which has higher value (Ba, 2544 ppm and Sr, 624 ppm). The average values of Rb, Li, Sn, Cs, Be, W and Ga are similarly higher than average crustal abundances while Nb and Ta are low. However, their values in the metasomatized muscovite-biotite gneiss which is in closer contact with the complex pegmatites shows higher values of Rb (754.9 ppm), Li (628 ppm), Sn (116 ppm), Cs (83.5 ppm), Be (20.61 ppm) and Ga (30 ppm) than the average values of other host rocks.

Pegmatites

The simple pegmatites (biotite-microcline-quartz pegmatites) and the complex pegmatites (albite-muscovite-quartz pegmatites) have SiO_2 contents > 70 wt% except sample CA13 of the complex pegmatite which has SiO_2 value of 64.12 wt%. Hence, the pegmatites are classified as granitic in composition and one syenite (Fig. 4a). The values of TiO_2, MnO, MgO, CaO and P_2O_5 are generally low (< 1 wt%) across the pegmatites compared to the migmatitic gneiss and the muscovite-biotite-gneiss host rocks. Conversely, the values of Al_2O, Na_2O and K_2O in the pegmatites are generally higher than the migmatitic gneiss and muscovite-biotite gneiss host rocks. The alumina saturation index also show that the pegmatites in Wamba area are strongly peraluminous (A/CNK = 1.39–1.53 in simple pegmatites and 1.26–2.26 in complex pegmatites).

Ba and Sr values in the pegmatites (Ba, 24–376 ppm; Sr, 141 ppm in simple pegmatites; and Ba, 19–501 ppm; Sr, 26–172 ppm in complex pegmatites) are lower compared to the migmatitic gneiss and muscovite-biotite gneiss. In contrast,

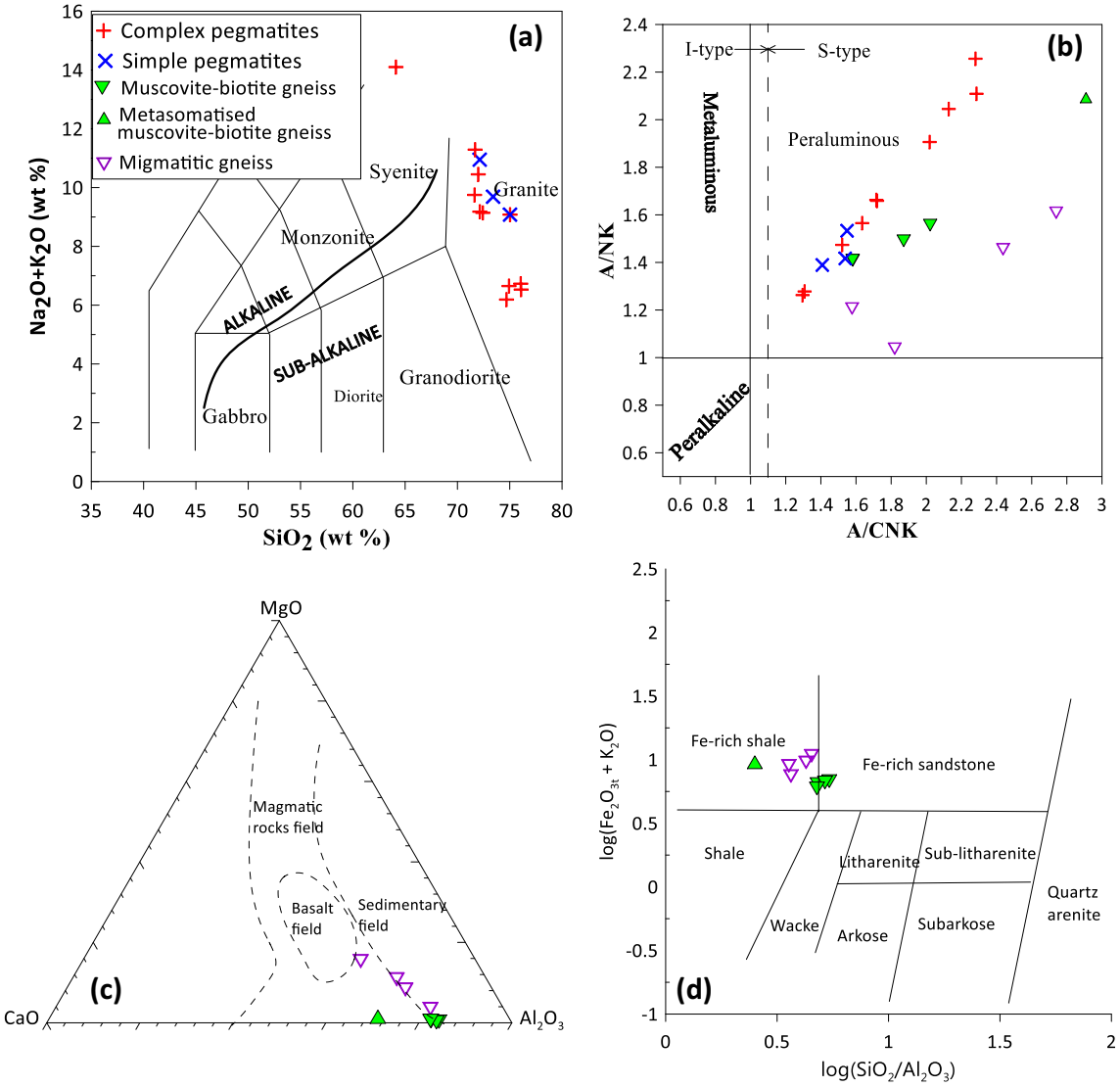

Fig. 4 **a** Total alkali versus silica diagram for the pegmatites. Divided fields from Gillespie and Style (1999); **b** Shand index plot for the host rocks and pegmatites in Wamba. A/NK = $Al_2O_3/(Na_2O+K_2O)$ and A/CNK = $Al_2O_3/(CaO+Na_2O+K_2O)$ after Maniar and Piccoli (1989); **c** MgO-CaO-Al_2O_3 ternary diagram of the host rocks after Leyreloup et al. (1977); **d** $\log(SiO_2/Al_2O_3)$ vs $\log(Fe_2O_3/K_2O)$ after Herron (1988) for discrimination of sedimentary protoliths. Symbols are as shown

the values of Rb, Sn, Cs, Be, Nb and Ta in the pegmatites (especially complex pegmatites) are several times higher than the migmatitic gneiss and muscovite-biotite gneiss and average crustal abundance. The concentrations of these elements in the complex pegmatites vary from wall zones to core zones but the intermediate zones and core zones indicate higher values of the elements (Table 1). The intermediate zone shows higher range of values for Rb (464.8–1719.9 ppm), Cs (16–32 ppm) and Be (75.83–527.88 ppm), while the core zone shows higher values for Sn (23–4466 ppm), Nb (24–106 ppm) and Ta (4.3–45 ppm) comparable to concentrations of average fertile granitic pegmatites of Superior Province of Černý and Meintzer (1988) and Selway et al. (2005). The values of Li across the complex pegmatites range from 20 to 161 ppm with the core zone and the wall zone of the complex pegmatites having the highest and the lowest values, respectively. The values of Ce, Cr, Co, Ni, Cu, Th, Mo, Pb and Zr are depleted in the pegmatites compared to the host rocks.

High peraluminous characteristics of the pegmatites and their host (migmatitic gneiss and muscovite-biotite gneiss) in Wamba area is shown on the $Al_2O_3/(Na_2O+K_2O)$ against $Al_2O_3/(CaO+Na_2O+K_2O)$ variation diagram of Maniar and Piccoli (1989); Fig. 4b). The complex pegmatites are most

Fig. 5 Harker's variation diagrams of major oxides and trace elements showing relationship between the pegmatites and the host rocks. Red cross sign, complex pegmatites; blue x sign, simple pegmatites; green inverted shaded triangle, muscovite-biotite gneiss; shaded green triangle, metasomatized muscovite-biotite gneiss; purple inverted open triangle, migmatitic gneiss

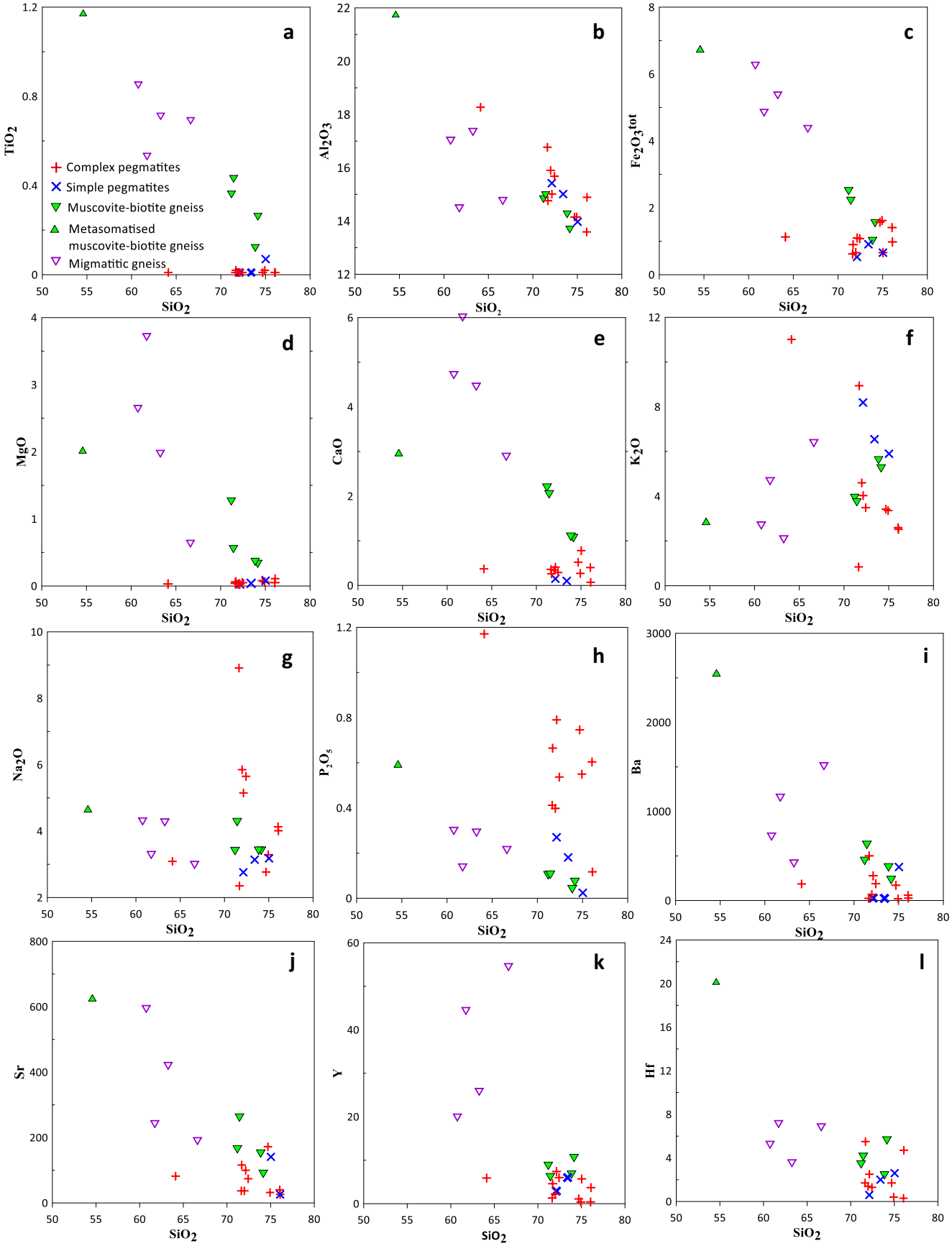
a
b
c
d
e
f
g
h
i
j
k
l
TiO2
Al2O3
Fe2O3tot
MgO
CaO
K2O
Na2O
P2O5
Ba
Sr
Y
Hf
SiO2
Complex pegmatites
Simple pegmatites
Muscovite-biotite gneiss
Metasomatised muscovite-biotite gneiss
Migmatitic gneiss

evolved having higher ratios of A/NK followed by muscovite-biotite gneisses and migmatitic gneisses. The rocks present S-type sedimentary source as shown in Fig. 4a. Figure 4 c and d further show that the host rocks are predominantly sedimentary in origin of iron-rich shale. This is consistent with Goodenough et al. (2014) findings on character of basement rocks in northcentral Nigeria. However, metaluminous host rocks and pegmatites have been accounted for in southwestern Nigeria by Matheis (1987).

The major oxides TiO_2, Al_2O_3, Fe_2O_3(t), MgO and CaO (Fig. 5a–e) showed negative correlation against SiO_2; Na_2O, K_2O and P_2O_5 showed scattered patterns (Fig. 5f–h), while trace elements Ba, Sr, Y and Hf (Fig. 5i–l) also show negative correlation against SiO_2 in the host rocks. Similarly, the concentrations of TiO_2, Al_2O_3, Fe_2O_3(t), MgO and CaO and trace elements Ba, Sr, Hf, Y and Zr (Fig. 5) indicate negative correlation with SiO_2, while Na_2O, K_2O and P_2O_5 showed scattered patterns (Fig. 5) in the pegmatites. This correlations show that the pegmatites could be related to the host rocks possibly by partial melting. The muscovite-biotite gneisses show that they are more evolved than the migmatitic gneisses (Fig. 5). The metasomatized muscovite-biotite gneiss which often exhibits anomalous character could be due to metasomatic changes in the rocks by hydrothermal fluid interactions resulting from the pegmatite melt. The erratic behaviour of Na_2O, K_2O and P_2O_5 of the pegmatites (Fig. 5f–h) probably shows incorporation of other rock materials into the melt from the protolith.

The trace element composition varies across the rock types (Table 1). Selected trace elements and REEs were normalized to primitive mantle and CI chondrites, respectively, according to McDonough and Sun (1995); Fig. 6 a and b). The patterns show that the migmatitic gneisses and muscovite-biotite gneisses are enriched in Cs, Rb, Th, K, La, Pb, U and Li and depleted in high field strength elements (HFSE; Nb, Ta, Hf and Ti), Ba, Sn and P (Fig. 6a). The metasomatized muscovite-biotite gneiss sample shows relatively higher enrichment in LILE and La, Nd, U and Li than the migmatitic gneisses and muscovite-biotite gneisses. Similarly, the pegmatites also show enrichments in Cs, Tl, Rb, Sn, K, Ta, Pb, U and Li (Fig. 6a). The enrichment of LILE and depletion of HFSE with few exceptions are generally the signatures of the Pan-African orogenic rocks in northern Nigeria (Goodenough et al. 2014; Akoh et al. 2015; Chukwu and Obiora 2021b). REE patterns (Fig. 6b) indicates inclined pattern with enrichment in the LREE compared to HREE. This is obvious in the host rocks pattern and from the ratios (La/Yb)n which range from 2.83 to 10.94 in migmatitic gneisses and 11.77–32.61 in muscovite-biotite-gneisses (Table 1). The rocks generally indicate mild negative Eu anomaly with Eu/Eu* = 0.35–0.92 except sample CA18 of muscovite-biotite-gneiss and the metasomatized muscovite-biotite gneiss which have Eu/Eu* values of 1.32 and 1.22, respectively.

Further consideration of the multi-element patterns (Fig. 6a), the pegmatites show more erratic signatures and more enriched in Cs, Tl, Rb, Sn, K, Ta, U and Li than the migmatitic gneiss and muscovite-biotite gneiss host rocks probably due to internal fractionation within the pegmatites. Similarly, they are depleted in Ba, Th, Nb, Pb, Nd, Hf, Ti and REEs than the host rocks. The enrichments in Sn, Ta and relatively Nb and depletion of La and Nd in the complex pegmatites contrary to the migmatitic gneiss and muscovite-biotite gneiss are attributed to mineralization of the pegmatites. REEs in the pegmatites are strongly depleted compared to the migmatitic gneiss and muscovite-biotite gneiss host rocks, and most of the HREEs (Tb, Ho, Tm and Lu) in the complex pegmatites

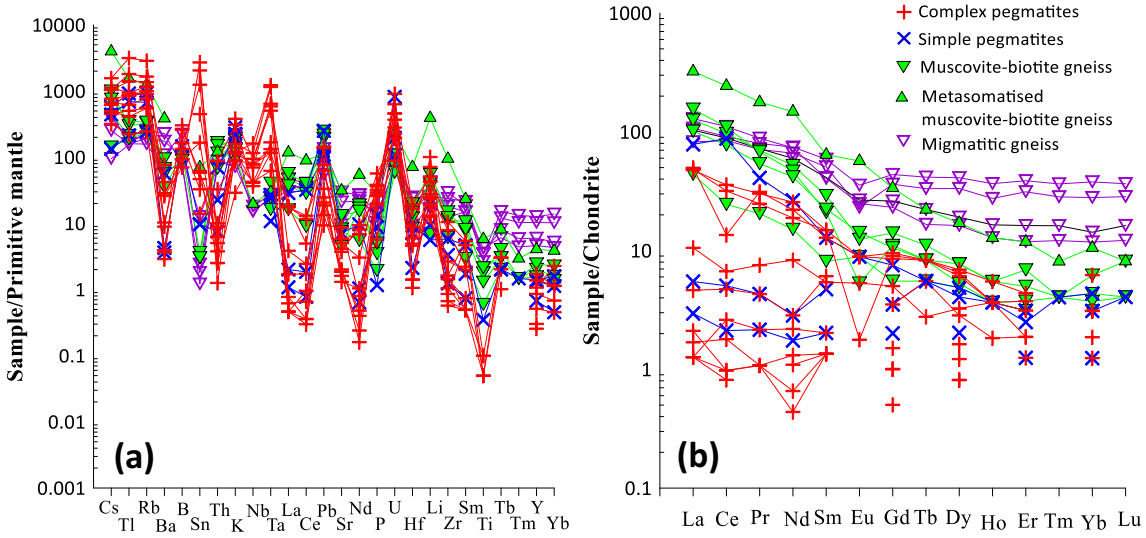

Fig. 6 **a** Primitive mantle-normalized spider diagrams for the muscovite-biotite gneiss, migmatitic gneiss host rocks and pegmatites; **b** Chondrite-normalized rare earth elements diagrams for the muscovite-biotite gneiss, migmatitic gneiss host rocks and pegmatites. Normalized after McDonough and Sun (1995) factor. Symbols are as shown. Normalized after McDonough and Sun (1995) factor. Symbols are as shown

are below detectable limit of 0.1 ppm (Fig. 6b). Similar to the host rocks, LREE concentrations (1.5–90.2 ppm; ∑LREE) in the pegmatites are higher than HREE concentrations (0.2–5.4 ppm; ∑HREE). This is also reflected in (La/Yb)n ratios which range from 1.26 to 25.0. Although most of the Eu in the pegmatites are below detectable limit of 0.1 ppm, available Eu values show negative anomaly with Eu/Eu* values range from 0.15 to 0.9 for the pegmatites.

Discussion

Sources and petrogenetic implications

Considering available and recent geochronological data of pegmatites in Nigeria (560–450 Ma; Matheis and Caen-Vachette 1983; Matheis 1987; Melcher et al. 2015) vis-a-vis the Pan African granites (640 – 535 Ma; Umeji and Caen-Vachette 1984; Dada and Respaut 1989; Goodenough et al. 2014), the age gap between these two events present their cogenetic relationship earlier advocated as controversial. Furthermore, the crystallization duration models for LCT pegmatites indicate that pegmatite dyke's crystallization does not take millions of years rather within days, weeks or thousands of years depending on the dyke's thickness (Baker 1998; London 2008; Bradley et al. 2017). This model and about 80 Ma gap between the pegmatites and the Pan African granites suggest that they are not likely to represent single event. Therefore the pegmatites in Wamba area are not likely to represent the end fraction of the crystallization of the Pan African granites around northcentral basement as earlier suggested by Jacobson and Webb (1946) and Kuster (1990). Although the field studies of this present work indicate some discordant and sharp contacts relationship between the pegmatites and the migmatitic gneiss and muscovite-biotite gneiss (host rocks) in some locations, however, the mineralogical and geochemical characteristics indicate that the pegmatites were likely generated by partial melting of the crustal pelitic protolith, perhaps the host rocks (Fig. 6a and b). Matheis and Caen-Vachette (1983) and Umeji and Caen-Vachette (1984) have shown that high Sr-initial ratios (0.710–0.723) of post-magmatic intrusions strongly indicate crustal influence in generation of the rocks. The presence of euhedral to subhedral garnet with inclusions in the study pegmatites also shows partial melting of pelitic sediments (Whitwort 1992). The linear trends between the pegmatites and the migmatitic gneiss and the muscovite-biotite gneiss (Fig. 5) also suggest that they are possibly related by partial melting of the host rocks. The similarity between the spidergram patterns (Fig. 6a) of the pegmatites and host rocks such as enrichments in Cs, Tl, Rb, K, Pb, U and Li and depletion in Ba, Nb, Hf and Ti also support relationship of the pegmatites possibly by partial melting of the host rocks. The differences in the patterns of the pegmatites and the host rocks such as higher enrichment in Rb, Sn, Ta, Li and P and depletion in Th and REEs in the complex pegmatites (Fig. 6a) can be attributed to influence of flux components in concentrating rare-metal minerals (cassiterites, Nb-Ta oxides and phosphates) in the complex (rare-metal) pegmatites.

The enrichment of large ion lithophile (LIL) elements (Cs, Rb, Th, K, Pb and U) and depletion of Nb-Ti and HREE especially in the host rocks (Fig. 6a) relative to primitive mantle are signatures of continental crust-derived melts. These elements are highly incompatible in the mantle minerals and hence accumulate more in the continental crust (Wedepohl 1995). The enrichment in LREEs relative to HREEs and Eu negative anomalies (Fig. 6b) in the pegmatites and host rocks also indicate generation relationship.

From the mineralogy and geochemical signatures in the complex pegmatites such as low REEs, LREEs > HREEs (Fig. 6b), low mafic elements (MgO and Fe_2O_{3tot}), enrichment in Cs, Rb, Sn, Ta, Pb, U and Li and depletion in Ba, Hf and Ti (Fig. 6a), they are in agreement with Shaw et al. (2016) on rare-metal pegmatites of LCT (Li-Ce-Ta) classification and S-type sedimentary origin. The formation of such high peraluminous pegmatites in high-grade metamorphic terrain (migmatite-gneiss complex) can be explained that partial melting most likely occurred at depth and the resulting melts form lenses; further internal fractionation within the pegmatites with additional hydrothermal fluids then rise to occupy the fractured spaces as dykes and sills. Several studies such as Ballouard et al. (2016), Simmons et al. (2016), Shaw et al. (2016), Fuchsloch et al. (2018) and Steiner (2019) in different part of the world have also proved pegmatites generation by partial melting and anatexis.

Experiments have indicated that peraluminous granites/pegmatites with high or low ratios of Nb/Ta can be produced by partial melting of metapelites bearing biotites + muscovite and titanium oxides depending on the temperature (Stepanov et al. 2014; Ballouard et al. 2016). Biotites host Li, Rb, Cs, Nb and Ta in metapelites with affinity for Nb over Ta (Shaw et al. 2016; Ballouard et al. 2016; Stepanov et al. 2014) and also source of H_2O, F and Cl, while titanium-bearing oxides have affinity for Ta over Nb (Stepanov et al. 2014). Therefore, low-temperature partial melting of metapelites generates melts with low Nb/Ta ratios due to complete destruction of ilmenites and residue biotites preferentially integrate Nb over Ta (Ballouard et al. 2016). However, there are evidences that internal fractional crystallization only within the pegmatites may not be sufficient to produce rare-metal abundances in peraluminous granite/pegmatites rather sub-solidus hydrothermal alteration combines with magmatic fractionation to concentrate Sn, W, Li, Cs, Nb and Ta (Ballouard et al. 2016; Steiner 2019). Fluid inclusions studies of pegmatites indicated that the transition from magmatic to hydrothermal conditions is gradational (London 1986) and the fluxing components

(H_2O, B, P and F) depress solidus temperature to about 350–550 °C and relatively low to moderate pressures (Sirbescu et al. 2008; Bradley et al. 2017). Ballouard et al. (2016) used whole-rock data to establish that K/Rb < 150, Nb/Ta < 5 and Zr/Hf < 18 values mark pegmatite-hydrothermal evolution signature and rare-metal mineralization. This occurs by increase in replacement of K by Rb in micas and feldspars, fractionation of Nb over Ta due to hydrothermal sub-solidus alterations thereby enriching Ta in F-rich residual melts which can result to secondary muscovitization, and increasing Kd values of Hf in zircon. All these will lead to diffusion of fluxing components which leads to fall in Ta solubility which concentrate rare metals in granites/pegmatites even adjacent country rocks. In this study, K/Rb < 100 in all the zones of complex pegmatites, Nb/Ta < 5 in the core zones, intermediate zones (CA12 and CA13) and a sample of the wall zone (CA6) while average ratios of Zr/Hf in all the zoned pegmatites are less than 18 except the simple pegmatites. Figure 7 shows that

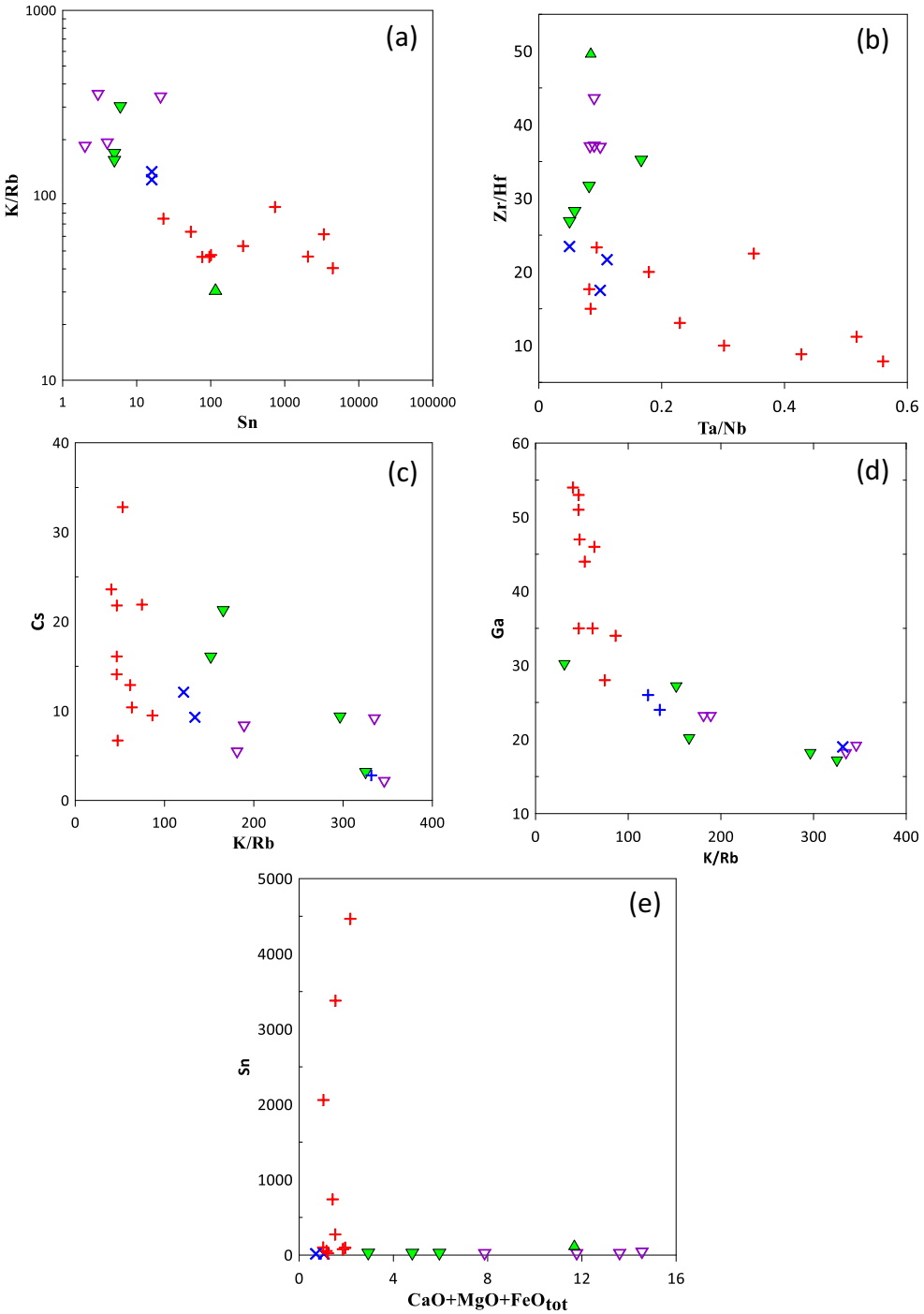

Fig. 7 Partial melting relationship between the pegmatites and the host rocks. **a** K/Rb vs Sn, **b** Zr/Hf vs Ta/Nb, **c** Cs vs K/Rb, **d** Ga vs K/Rb, **e** Sn versus the McKeough et al. (2013) hybridization factor. Symbols are as shown

partial melting and hydrothermal alteration process play some roles in the Wamba pegmatites generation. K/Rb vs Sn, Zr/Hf vs Ta/Nb, K/Rb vs Cs and K/Rb vs Ga (Fig. 7a–d, respectively) show partial melting relationships from the host rocks (migmatitic gneiss and muscovite-biotite gneiss) to the simple pegmatite and the complex pegmatites. These also indicate similar genetic relationship. The non-correlation of Sn with hybridization factor (CaO, MgO and FeO; Fig. 7e) indicates that the enrichment of Sn (up to 4466 ppm in pegmatites and 116 ppm in metasomatized muscovite-biotite gneiss) may not have originated during melting and assimilation of country rocks in early stage rather most probably enriched by hydrothermal processes at the later stage. This was earlier observed by McKeough et al. (2013) in Wollaston Domain, Canada, and Fuchsloch et al. (2018) in Cape Cross-Uis, Namibia.

Similarly, occurrences of rare-metal pegmatites by partial melting in high-grade metamorphic terrains abound around the world although with higher Li and Ta concentrations than Wamba pegmatites. Such works are observed in Lewisian rare-metal pegmatites, Scotland (Shaw et al. 2016); Cape Cross-Uis pegmatites, Namibia (Fuchsloch et al. 2018); Mt. Mica pegmatites, USA (Simmons et al. 2016); and the Sveconorwegian Pegmatite Province (Müller et al. 2017).

Potential mineralizations

Certain geochemical factors can be used to determine the degree of fractionations in granites and pegmatites for possible rare metal exploration. Apart from other advanced exploration techniques for LCT pegmatite mineralization, recent works indicated that whole-rock geochemistry maintain a critical tool in grassroots exploration (Cerný 1989; Dimmell and Morgan 2005; Selway et al. 2005; Steiner 2019). The study rocks in Wamba area which are strongly peraluminous with the complex pegmatites having the highest A/CNK values of 1.26–2.24 are comparable to highly fertile granites/pegmatites (A/CNK > 1.2) of Selway et al. (2005). The complex pegmatites are enriched in Li, Rb, Be, Nb, Cs, Ta, Ga, Sn and W (intermediate and core zones have highest concentrations) and depleted in Ti, Sr, Ba and Zr relatively comparable to known LCT pegmatites but still lower compared to Tanco pegmatites, Canada; Greenbush pegmatites, Australia; and Altai pegmatites, China. The metasomatized muscovite-biotite gneiss host rock is also enriched in Li, Rb, Be, Cs, Ga, Sn and W, while the migmatitic gneiss and muscovite-biotite gneiss host rocks are only relatively enriched in tungsten (W). These show that the host rocks could serve as pointer to the mineralized zone. Considering the variation diagrams K/Rb against Rb (Fig. 8a), the complex pegmatites and metasomatized muscovite-biotite gneiss plot as mineralized while the simple pegmatites and the migmatitic gneiss and muscovite-biotite gneiss host rocks plot as non-mineralized. The average ratios of K/Rb, Mg/Li, K/Cs and Nb/Ta (Table 2) in fertile granites/pegmatites are expected to be very low than average upper continental crust (252, 30, 7630 and 11.4 respectively) of Taylor and McLennan (1985) and Cerný (1989). The average ratios of K/Rb, Mg/Li, K/Cs, Zr/Hf and Nb/Ta in the complex pegmatites are 56.69, 6.90, 2108.9, 14.94 and 5.68, respectively, comparable to bulk elements in fertile pegmatites of Selway et al. (2005). The ratios of the elements also vary relatively within the zones of the complex pegmatites such that the core zones show least average values of Nb/Ta (3.55), Mg/Li (5.27) and Zr/Hf (13.28); intermediate zones show least average values of K/Rb of 48.18, while the wall zones show the least values of K/Cs of 1526.3. These indicate internal fractionations within the complex pegmatites which increase differentiation from albite wall zone to spodumene-quartz core zone. The average values of K/Rb, Mg/Li, K/Cs, Zr/Hf and Nb/Ta in the metasomatized muscovite-biotite gneiss are

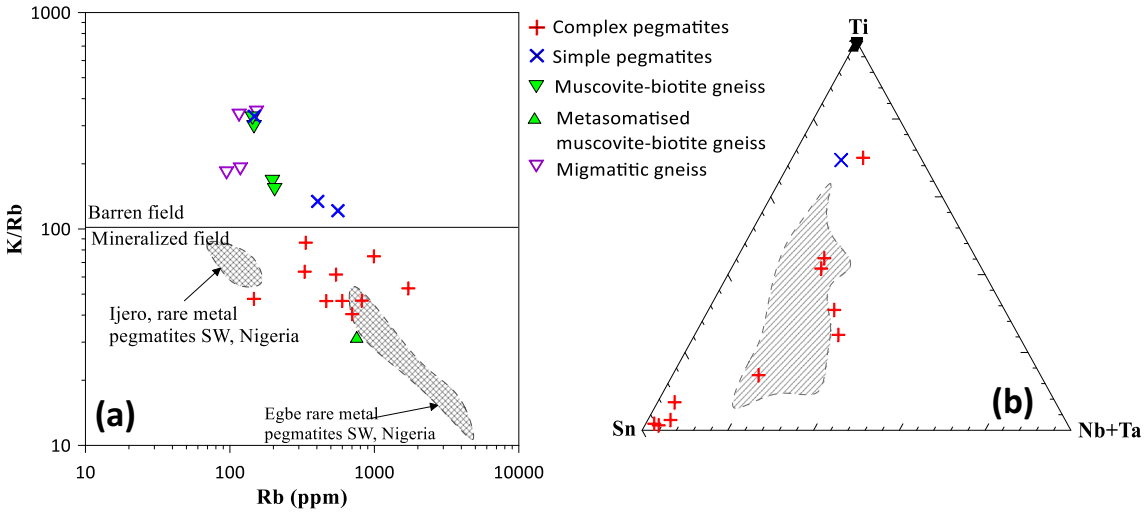

Fig. 8 Mineralization of the pegmatites. **a** Rb versus K/Rb showing the division between barren and mineralized pegmatites (Stavrov et al. 1969); **b** Ti-Sn-(Nb + Ta) ternary plot for the pegmatites and host rocks. Symbols are as shown

Table 2 Trace elements ratios in the Wamba pegmatites and host rocks compared with fertile granites

Host rocks		K/Rb	K/Cs	Nb/Ta	Mg/Li	Zr/Hf
Biotite-gneisses	Range	181.25–346	4307–26440	10.0–12.0	92.6–828.7	36.7–43.3
	Mean	262.8	9178.4	11	338.2	38.4
Muscovite-biotite gneisses	Range	151–325	1947–15523	6–13.3	22–197	26.7–35
	Mean	234.8	5936	9.9	100.8	30.2
Metasomatized gneiss	Mean	31.12	281.35	11.81	19.30	49.60
Pegmatites						
Simple pegmatite	Range	121–331	5619–17492	9.0–20.0	5.6–53.6	17.5–23.4
	Mean	195.7	9652	13	25.1	20.8
Complex pegmatites (wall zone)	Range	47.5–63.5	1040–2011	3.3–12	11.4–15	10–17.7
	Mean	55.5	1526	7.7	13	13.8
Complex pegmatites (intermediate zone)	Range	46.4–53.14	1530–2786	1.78–11.9	3.1–9.04	7.8–23.3
	Mean	48.1	1950.1	5	5.3	17.1
Complex pegmatites (core zone)	Range	40.4–86.5	1203–3388	1.93–5	2.9–7.5	8.8–20
	Mean	65.7	2558	3.5	5.2	13.2
*UCC	Mean	252	7630	11.4	--	
*Fertile granite	Range	42–270	1600–15400	--	1.7–50	14–64

*Fertile peg. Ratios data from Cerný (1989)

*UCC represents average upper-continental crust after Taylor and McLennan (1985)

31.12, 19.30, 281.35, 49.60 and 11.82, respectively, while the average values in the simple pegmatites are 195.7, 25.11, 9652.8, 20.88 and 13.0, respectively. The relationship between Sn, Nb and Ta (Fig. 8b) is comparable to the findings of Kuster (1990) and shows that cassiterite is the dominant mineral mined around the locality of Mararaba Gwongwon, Maramara and Wuji areas of Wamba by artisanal miners.

Generally as shown in Table 2 and Fig. 7, the partial melting is from the migmatitic gneiss to muscovite-biotite gneiss to metasomatized muscovite-biotite gneiss to more fertile complex pegmatites. These ratios obtained for the studied pegmatites are within the range found in muscovites in rare-metal pegmatites in southwestern and northcentral Nigerian Basement complex by Cerný (1989), Matheis (1987), Kuster (1990) and Chukwu and Obiora (2021b). But they are mineralogically and geochemically relatively less evolved especially in Ta, Li and Cs compared to some rare-metal pegmatites in Nigeria (Keffi area, Akoh et al. 2015) and the world known LCT pegmatites such as Tanco, Canada (Černý and Ercit 2005); Greenbush, Australia (Kesler et al. 2012); and Altai, China (Zhu et al. 2006). However, the values of cassiterite (Sn, up to 4466 ppm) are predominant compared to Ta and Nb in the Wamba area and also more than the southwestern Nigeria and Keffi area pegmatites. The Wamba area accounted for most of the mined minerals recorded by Jacobson and Webb (1946) in Nigeria in twentieth century.

Trace element equilibrium batch melting (EBM) modelling

Considering the field, mineralogical and geochemical characteristics of the rocks which show possible anatectic relationship between the pegmatites and the host rocks (muscovite-biotite gneiss), equilibrium batch melting petrogenetic modelling (Shaw 1970) was applied to further test their generation. Field and petrographic studies show that the pegmatites are in situ and remained in equilibrium with the residue until final melting. Therefore, it matches the batch melting process of Shaw (1970), Ersoy (2013) and Saki et al. (2021). To model the trace element modal equilibrium batch melting, Shaw (1970) equation for batch melts was applied:

$$C_L = \frac{C_0}{D_0 + F(1-D_0)}$$

where C_L is the calculated element concentrations in the melt for a given degree of partial melting, C_0 is the element concentration in the protolith (source), F is the fraction of the melt produced during anatexis and D_0 is the calculated bulk mineral/melt partition coefficient for the chosen element. Considering the primary assemblage of the source (muscovite-biotite gneiss) rock which is dominated by k-feldspar/plagioclase and biotite, EBM-models were calculated for Pb versus Rb/Pb following White et al. (2009), Lucci et al. (2016) and Saki et al. (2021). The bulk partition coefficients (D_{Rb} and D_{Pb}) of the element were calculated following the method proposed by White (2003) and Saki et al. (2021). Mineral/melt partition coefficients were adopted from existing literatures (Philpotts and Schnetzler 1970; Nash and Crecraft 1985; Bea et al. 1994; Icenhower and London 1996) through the GERM K_D database (https://earthref.org/GERM/). The results are presented in Table 3.

Table 3 Trace elements modal batch melting (EBM) model for the pegmatites

Model C_L		Partition coefficients		
		D_{Rb}	D_{Pb}	
		0.84	1.53	
		Rb	Pb	Rb/Pb
Source (C_0) (ppm)	Avg CA1-C19	146.52	23.27	6.29
Batch melt (C_L) (ppm)				
F:	0.9	148.91	22.10	6.74
	0.8	153.83	19.99	7.70
	0.7	161.59	17.24	9.37
	0.6	172.63	14.23	12.13
	0.5	187.65	11.25	16.68
	0.4	207.57	8.53	24.33
	0.3	233.75	6.22	37.56
	0.2	268.07	4.37	61.33
	0.1	313.16	2.96	105.82
	0.01	372.10	1.94	191.72

F represent the proportion of batch melt

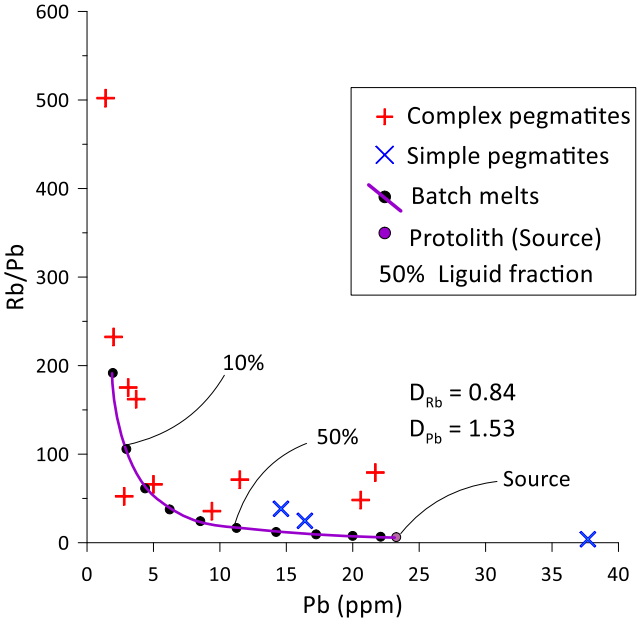

Fig. 9 Pb versus Rb/Pb diagram showing the genesis of the pegmatites via equilibrium batch melting (EBM) of the muscovite-biotite gneisses. Bulk rock/melt partition coefficients for the EBM-models are shown in the diagram. The calculated EBM-curve stands for the Shaw (1970) modal batch melting calculated for K_D. the percentages stand for the amount of liquid fraction. Symbols as shown

The equilibrium batch melt hypothesis was applied for all the pegmatites (n = 13), assuming the average composition of the host rocks (CA1-CA19) with the exception of sample CA22 represent the protolith source before partial melting activity. The major element EBM modelling was estimated for Rb and Pb. The calculated bulk partition coefficients (K_D) are D_{Rb} = 0.84 and D_{Pb} = 1.53 for rock type dacite-rhyolite/granite. The results of the EBM modelling were presented in Table 2 and Fig. 9. The curve (Fig. 9) for the calculated batch melts shows that the pegmatites have similar trend with the calculated batch melts and confirm the pegmatite as product of the modal batch melting with predominantly less than 1–50% degree of partial melting of the muscovite-biotite gneiss and sparse 80% degree of partial melting. Christiansen and Keith (1996) has shown that larger degrees (large F) of partial melting cause decrease in incompatible elements in the daughter melt in partial melting processes. The predominantly low degree (F < 0.5) of partial melting of biotite from the source rock in this study (Fig. 9) results to the production of melts enriched in incompatible elements such as Rb and Nb and depleted in compatible elements in the pegmatites compared to the source rock.

Tectonic implications

Collision settings (continent-continent) are characterized by extensive high-grade metamorphism, compressional deformations and magmatism (Stammeier et al. 2015). This setting is associated with different tectonic processes such as subduction of continental crust, crustal thickening, late-post orogenic collapse and premature within-plate setting (Pearce 1996). The study area lies within the eastern terrain of northcentral Nigeria (Ajibade et al. 1987; Ferré et al. 2002) that is characterized by high-grade migmatitic metamorphic rocks. The migmatitic rocks have Paleoproterozoic protoliths that were migmatized during Neoproterozoic Era (Ajibade et al. 1987; Ferré et al. 2002). The Neoproterozoic tectono-metamorphic events were described as monocyclic collision-related events that comprise of the D_1 tectonic event (E-W thrusting) and D_2 characterized by N-S to NNE-SSW deformation thrusting (Ferré et al. 2002). The elemental signatures of the studied rocks (granitic pegmatites and host rocks) such as enrichment in LIL elements and the depletion of HFS elements (Fig. 6) especially in the host rocks show a crustal-related collision settings (Pearce 1996). The strongly peraluminous characteristics (Fig. 4 b, c and d) of the rocks also suggest metasediment protoliths similar to orogenic settings of Alpine-Himalayan type. The paragneisses plot predominantly in the field of active continental margin in SiO_2-K_2O/Na_2O diagram of Roser and Korsch (1988) (Fig. 10). Nd model ages and Pb upper intercept ages of migmatites in northern Nigeria show that they were derived from 2.0 to 1.8 Ga metasediment protoliths (Dada et al. 1993). The migmatitic gneiss and muscovite-biotite gneiss host rocks in the study area probably represent crustal sediments emplaced during the Paleoproterozoic Era but deformed and migmatized by syn-collision during the late Neoproterozoic Pan-African

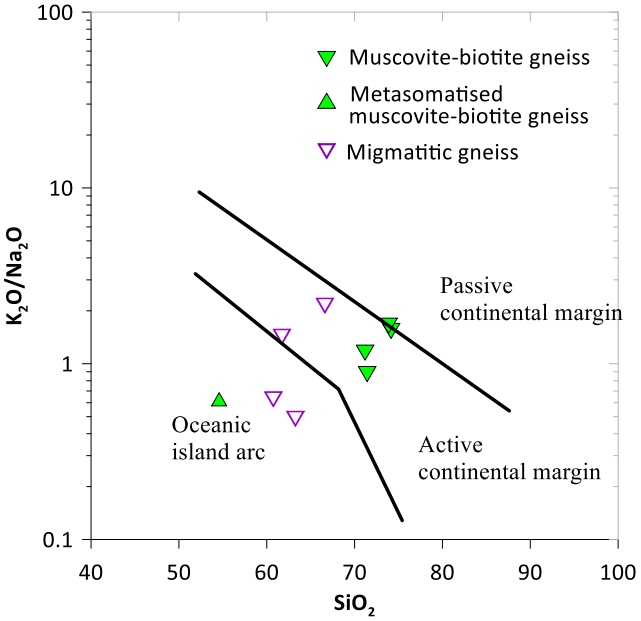

Fig. 10 (**a**) SiO_2 vs K_2O/Na_2O diagram for tectonic discrimination of the metasediments (host rocks) after Roser and Korsch (1986). Symbols are as shown

orogeny. Brito Neves et al. (1995) have also shown that gneisses of similar age in Borborema Province were deformed by similar Brasiliano event. The active continental margin of the host rocks and the post-collision of the northcentral pegmatites (Goodenough et al. 2014; Chukwu and Obiora 2021b) further show that the pegmatites came as reactivated and partial melting of the high-grade metasediments at depth during the Pan-African orogeny. The host rocks in the study area is similar to the Cordilleran suits in western USA (Frost et al. 2001), while the pegmatites is equivalent to post-collision pegmatites in southern Sinai, Egypt (Abdelfadil et al. 2016), the rare-metal pegmatites of Lewisian gneiss complex, northwest Scotland (Shaw et al. 2016) and other LCT, Sn and W pegmatites of the world which are known to predominantly occur within reactivated continent-continent collision zones.

Generally, the setting that formed the basement complex is related to the orogenic activities at the continental arc of the Tuareg Shield and subsequent continent-continent collision with passive continental margin of the West African craton during the Pan-African events which led to the occurrence of the pegmatites. Several authors have similar tectonic findings for Nigerian basement complex such as Ferré et al. (2002), Obiora and Ukaegbu (2009) and Goodenough et al. (2014)

Conclusion

The field, mineralogy and geochemical study of the Wamba pegmatites show that they are predominantly cassiterite dominated complex (rare-metal) pegmatites and rarely massive simple pegmatites hosted by high-grade metamorphic rocks (migmatitic gneisses and muscovite-biotite gneisses). The pegmatites are partly zoned as albite-tourmaline wall zone, albite-beryl intermediate zone and quartz-spodumene core zones. The complex pegmatites have dominant minerals, albite, muscovite and quartz. Accessory minerals include microcline, garnets, tourmaline, beryl, spodumene and cassiterite-neobium-tantalite minerals. The pegmatites and the host rocks are highly peraluminous and S-type saturated sources. The complex pegmatites exhibit low K/Rb, Nb/Ta, Mg/Li and Zr/Hf mostly within the core and intermediate zones than the wall zone and enriched in Rb, Li, Cs, Be, Sn, W, Nb and Ta than the simple pegmatites and migmatitic gneisses and muscovite-biotite gneisses. The geochemical signatures of the pegmatites are similar to the host rocks suggesting genetic relationship most probably by anatexis and remobilization of the high-grade metasedimentary rocks deeper than the present erosion surface. The rare elements in the pegmatites are formed by low-temperature partial melting of pelitic protolith combined with hydrothermal processes. The modal equilibrium batch melting estimations strongly affirm genesis from the muscovite-biotite gneisses in support of the recent determined age of the northcentral pegmatites which show that they are not likely related to the Pan-African granites as earlier advocated. The host, migmatitic gneisses and muscovite-biotite gneisses are related to continent-continent collision at the active continental margin of the Tuareg Shield with the passive continental margin of the West African craton accompanied by deformations, reactivation and reworking led to the emplacement of the peraluminous pegmatites.

Acknowledgements We are thankful to the Association of Applied Geochemists (AAG) for their sponsorship of the whole rock geochemical analyses (In-Kind Analytical support) as parts of the first authors Ph.D research work. The quality and detailed analyses of the Staff of Genalysis (Intertek) Laboratory Services, Australia, are highly appreciated. We are indebted to Prof. T. C. Davies for his expert dispositions that resulted to the success of the AAG support for the geochemical analyses. Efforts of the editors Abdullah M. Al-Amri and Federico Lucci and other anonymous reviewers are highly appreciated for their constructive insights and comments that improve the paper.

Availability of data and material No restriction on the availability of data and material

Code availability No restrictions

Funding The geochemical analysis was sponsored by the Association of Applied Geochemists (AAG), In-Kind Analytical support as parts of the first authors Ph.D research work.

Declarations

Conflict of interest The authors declare that they have no competing interests.

References

Abdelfadil KM, Asimow PD, Azer MK, Gahlan HA (2016) Genesis and petrology of Late Neoproterozoic pegmatites and aplites associated with the Taba metamorphic complex in southern Sinai, Egypt. Geochem Acta 14(3):219–233

Ajibade AC, Wright JB (1989) The Togo–Benin–Nigeria Shield: evidence of crustal aggregation in the Pan-African belt. Tectonophysics 165:125–129

Ajibade AC, Woakes M, Rahaman MA (1987) Protorozoic crustal development in the Pan-African regime of Nigeria. In: Kroner A (ed) Proterozoic lithospheric evolution, vol 17. American Geophysical Union, Washington DC, pp 259–271

Akintola OF, Adekeye JID (2008) Mineralization potentials of pegmatites in the Nasarawa area of central Nigeria. Earth Sci Res J 12(2): 213–234

Akoh JU, Ogunleye PO, Aliyu AI (2015) Geochemical evolution of micas and Sn-, Nb-, Ta- mineralization associated with the rare metal pegmatite in Angwan Doka, central Nigeria. J Afr Earth Sci 97:167–174

Baker DR (1998) The escape of pegmatite dikes from granitic plutons - constraints from new models of viscosity and dike propagation. Can Mineral 36:255–263

Ballouard C, Poujol M, Boulvais P, Branquet Y, Tartèse R et al (2016) Nb-Ta fractionation in peraluminous granites: a marker of the magmatic–hydrothermal transition. Geol 44:231–234

Bea F, Pereira MD, Stroh A (1994) Mineral/leucosome trace-element partitioning in a peraluminous migmatite (a laser ablation-ICP-MS study). Chem Geol 117:291–312

Bradley DC, McCauley AD, Stillings LM (2017) Mineral-deposit model for lithium-cesium tantalum pegmatites. In: Scientific Investigations Report 2010–5070–O; US Geological Survey: Reston, WV, USA, 32p

Brito Neves BB, Van Schmus WR, Santos EJ, Campos Neto MC, Kozuch M (1995) O evento Cariris Velhos na Provı´ncia Borborema: integrac¸a˜o de dados, implicac¸o˜es e perspectivas. Revista Brasileira de Geocieˆncias 25:279–296

Burke KC, Dewey JF (1972) Orogeny in Africa. In: Dessauvagie TFJ, Whiteman AJ (editors) Africa geology. 1st ed. University of Ibadan Press, Ibadan, pp. 583–608

Cerný P (1989) Contrasting geochemistry of two pegmatite fields in Manitoba: products of juvenile Aphebian crust and polycyclic Archean evolution. Precambrian Res 45:215–234

Cerny P, Ercit TS (2005) The classification of granitic pegmatites revisited Canad Mineral 43:2005–2026

Černý P, Meintzer RE (1988) Fertile granites in the Archean and Proterozoic fields of rare element pegmatites: crustal environment, geochemistry and petrogenetic relationships. In: Recent advances in the geology of granite-related mineral deposits, vol 39. Can Institute of Mining and Metallurgy, Spec Publ, pp 170–206

Christiansen EH, Keith JD (1996) Trace element systematics in silicic magmas: a metallogenic perspective. In: Wyman DA (ed) Trace element Geochemistry of Volcanic rocks: applications for massive sulphide exploration: Geol Assoc Can Short Notes, vol 12, pp 115–151

Chukwu A, Obiora SC (2014) Whole-rock geochemistry of basic and intermediate intrusive rocks in the Ishiagu area: further evidence of anorogenic setting of the Lower Benue rift, southeastern Nigeria. Turk J Earth Sci 23:427–443

Chukwu A, Obiora SC (2018) Geochemical constraints on the petrogenesis of the pyroclastic rocks in Abakaliki Basin (Lower Benue Rift), Southeastern Nigeria. J Afr Earth Sci 141:207–220

Chukwu A, Obiora SC (2021a) Petrogenetic characterization of pegmatites and their host rocks in southern Akwanga, North-central Basement Complex, Nigeria. J Earth Syst Sci 130:18. https://doi.org/10.1007/s12040-020-01498-7

Chukwu A, Obiora SC (2021b) Petrogenesis and tectonomagmatic updates on the origin of the igneous rocks in the lower Benue rift, southeastern Nigeria. Arabian J Geosci 14: 154. https://doi.org/10.1007/s12517-021-06475-y

Dada SS, Respaut JP (1989) The quartz fayalite monzonite (bauchite) of Bauchi, new evidence of a syntectonic Pan-African magmatism in northern Nigeria. Comptes Rendus Academie Science de Paris 309: 887–892

Dada SS, Tubosun IA, Lancelot JR, Lar AU (1993) Late Archaean U-Pb Age for the reactivated basement of northeastern Nigeria. J Afr Earth Sci 16:495–412

Dimmell PM, Morgan JA (2005) The Aubry pegmatites: exploration for highly evolved lithium-cesium-tantalum pegmatites in northern Ontario. Explor Min Geol 14:45–59

Ersoy EY (2013) PETROMODELER (petrological modeler): a Microsoft R excel spreadsheet program for modeling melting, mixing, crystallization and assimilation processes in magmatic systems. Turk J Earth Sci 22(1):115–125

Ferré EC, Gleizes G, Caby R (2002) Obliquely convergent tectonics and granite emplacement in the Trans-Saharan belt of eastern Nigeria: a synthesis. Precambrian Res 114:199–219

Frost BR, Barnes CG, Collins WJ, Arculus RJ, Ellis DJ et al (2001) A geochemical classification for granitic rocks. J Petrol 42:2033–2048

Fuchsloch WC, PAM N, Kinnaird JA (2018) Classification, mineralogical and geochemical variations in pegmatites of the Cape Cross-Uis pegmatite belt, Namibia. Lithos 296:79–95

Gillespie MR, Style MT (1999) Rock classification Scheme volume 1, classification of igneous rocks, British Geological Survey Research Report, 2nd ed. British Geological Survey, Keyworth, Nottingham

Goodenough KM, Lusty PAJ, Roberts NMW, Key RM, Garba A (2014) Post-collisional Pan-African granitoids and rare metal pegmatites in western Nigeria: age, petrogenesis, and the 'pegmatite conundrum'. Lithos 200-201:22–34

Grant NK, Hickman MH, Burkholder FR, Powell JL (1972) Kibaran metamorphic belt in Pan-African Domain of west Africa. Nat Phys Sci 238:90–91

Herron MM (1988) Geochemical classification of ferruginous sands and shales from core or log data. J Sediment Petrol 58:820–829

Icenhower J, London D (1996) Experimental partitioning of Rb, Cs, Sr and Ba between alkali feldspar and peraluminous melt. Am Mineral 81:719–734

Jacobs J, Thomas RJ (2004) Himalayan-type indenter-escape tectonics model for the southern part of the late Neoproterozoic-Early Palaeozoic East African-Antarctic Orogen. Geol 32:721–724

Jacobson R, Webb JS (1946) The pegmatites of Central Nigeria. Geological Survey of Nigeria Bulletin 17, Kaduna

Jahns RH, Burnham CW (1969) Experimental studies of pegmatite genesis: I. A model for the derivation and crystallization of granitic pegmatites. Econ Geol 64:843–864

Kesler SE, Gruber PW, Medina PA, Keoleian GA, Everson MP et al (2012) Global lithium resources: relative importance of pegmatite, brine and other deposits. Ore Geol Rev 48:55–69

Kuster D (1990) Rare-metal pegmatites of Wamba, central Nigeria – their formation in relationship to late Pan – African granites. Mineral Deposita 25:25–33

Leyreloup A, Pupuy AC, Andrianbololona R (1977) Chemical composition and consequences of the French Massif Central Precambrian Crust. Contrib. Petrol 62:283–300

London D (1986) Magmatic hydrothermal transition in the Tanco rare-element pegmatite: evidence from fluid inclusions and phase-equilibrium experiments. Am Mineral 71:376–395

London D (2008) Pegmatites. The Can Mineral spec publ 10, 347p

Lucci F, Rossetti F, White JC, Moghadam HS, Shirzadi A, Nasrabady M (2016) Tschermak fractionation in calc-alkaline magmas: the

Eocene Sabzevar volcanism (NE Iran). Arab J Geosci 9:10. https://doi.org/10.1007/s12517-016-2598-0
Maniar PD, Piccoli PM (1989) Tectonic discrimination of granitoids. Geol Soc Am Bull 101:635–643
Matheis G (1987) Nigerian rare-metal pegmatites and their lithological framework. In: African Geology Reviews. Bowden P, Kinnaird JA (editors). Geol J 22:271–291
Matheis G, Caen-Vachette M (1983) Rb–Sr isotopic study of rare-metal bearing and barren pegmatites in the Pan-African reactivation zone of Nigeria. J Afr Earth Sc 1:35–40
McCurry P, Wright JB (1977) On place and time in orogenic granite plutonism. J Geol Soc Am 82(6):1713–1716
McDonough WF, Sun S-S (1995) The composition of the Earth. Chem Geol 120:223–253
McKeough MA, Lentz DR, CRM MF, Brown J (2013) Geology and evolution of the pegmatite-hosted U-Th ± REE-Y-NB mineralization, Kulyk, Eagle, and Karin Lakes region, Wollaston Domain, northern Saskatchewan, Canada: examples of the dual role of extreme fractionation and hybridization processes. J Geosci 58:321–346
Melcher F, Graupner T, Gabler H-E, Sitnikova M, Henjes-Kunst F et al (2015) Tantalum-(niobium-tin) mineralization in African pegmatites and rare metal granites: constraints from Ta-Nb oxide mineralogy, geochemistry and U-Pb geochemistry. Ore Geol Rev 64:667–719
Müller A, Romer RL, Pedersen R-B (2017) The Sveconorwegian pegmatite province—thousands of pegmatites without parental granites. Can Mineral 55:283–315
Nash WP, Crecraft HR (1985) Partition coefficients for trace elements in silicic magmas. Geochim Cosmochim Acta 49:2309–2322
Obiora SC, Ukaegbu VU (2009) Petrology and geochemical characteristics of Precambrian granitic basement complex rocks in the southernmost part of North-Central Nigeria. Chin J Geochem 28:377–385
Odeyemi I (1981) A review of the orogenic events in the Precambrian basement of Nigeria, West Africa. Geol Rundsch 70:897–909
Okunlola OA (2005) Metallogeny of Tantalum-Niobium mineralization of Precambrian pegmatites of Nigeria. Mineral Wealth 137:38–50
Okunlola AO, Ocan OO (2009) Rare metal (Ta-Sn-Li-Be) distribution in Precambrian pegmatite of Keffi area, central Nigeria. Nat Sci 7:90–99
Pearce JA (1996) Sources and setting of granitic rocks. Episodes 19:120–125
Philpotts JA, Schnetzler CC (1970) Phenocryst-matrix partition coefficients for K, Rb, Sr and Ba, with applications to anorthosite and basalt genesis. Geochim Cosmochim Acta 34(3):307–322. https://doi.org/10.1016/0016-7037(70)90108-0
Roser BP, Korsch RJ (1988) Provenance signatures of sandstone-mudstone suites determined using discriminant function analysis of major-element data. Chem Geol 67:119–139
Saki A, Lucci F, Miri M, White JC (2021) Trondhjemite leucosomes generated by partial melting of a hornblende gabbro (Alvand plutonic complex, Hamedan, NW Iran). Int Geol Rev. https://doi.org/10.1080/00206814.2020.1861554
Selway JB, Breaks FW, Tindle AG (2005) A review of rare-element (Li-Cs-Ta) pegmatite exploration techniques for the Superior Province, Canada, and large worldwide tantalum deposits. Explor Min Geol 14(1-4):1–30
Shaw GE (1970) A summary of lightning current measurements collected at Mount Lemmon, Arizona. J Geophys Res 75(12):2159–2164
Shaw RA, Goodenough KM, Roberts NMW, Horstwood MSA, Chenery SR, Gunn AG (2016) Petrogenesis of rare-metal pegmatites in high-grade metamorphic terranes: a case study from the Lewisian Gneiss Complex of north-west Scotland. Precambrian Res 281:338–362
Simmons WB, Foorf EE, Falster AU, King VT (1995) Evidence for an anatectic origin of granitic pegmatites, western Maine, USA. Geol Soc Am Abstr Programs 27(6):A411
Simmons W, Falster A, Webber K, Roda-Robles E, Boudreaux AP, Grassi LR, Freeman G (2016) Bulk composition of Mt. Mica pegmatite, Maine, USA: implications for the origin of an LCT type pegmatite by anatexis. Can Mineral 54:1053–1070
Sirbescu M-LC, Hartwick EE, Student JJ (2008) Rapid crystallization of the Animikie Red Ace pegmatite, Florence County, northeastern Wisconsin—inclusion microthermometry and conductive-cooling modeling. Contrib Mineral Petrol 156:289–305
Stammeier J, Jung S, Romer RL, Berndt J, Garbe-Schönberg D (2015) Petrology of ferroan alkali-calcic granites: synorogenic high-temperature melting of undepleted felsic lower crust (Damara orogen, Namibia): Lithos 224: 114–125. doi:10.1016/j.lithos.2015.03.004
Stavrov OD, Stolyarov IS, Iocheva EI (1969) Geochemistry and origin of the Verkh-Iset granitoid massif in central Ural. Geochem Int 6:1138–1146
Steiner BM (2019) Tool and workflows for grassroots Li-Cs-Ta (LCT) pegmatite exploration. Minerals 9:499. https://doi.org/10.3390/min9080499
Stepanov AA, Mavrogenes J, Meffre S, Davidson P (2014) The key role of mica during igneous concentration of tantalum. Contrib Mineral Petrol 167:1–8
Taylor SR, McLennan SM (1985) The continental crust; its composition and evolution; an examination of the geochemical record preserved in sedimentary rocks. Blackwell
Umeji AC, Caen-Vachette M (1984) Geochronology of Pan-African Nassarawa-Eggon and Mkar-Gboko granites, southeast Nigeria. Precambrian Res 23:317–324
Wedepohl KH (1995) The composition of the continental crust. Geochim Cosmochim Acta 59:1217–1232
White JC (2003) Trace-element partitioning between alkali feldspar and peralkalic quartz trachyte to rhyolite magma. Part II: Empirical equations for calculating trace-element partition coefficients of large-ion lithophile, high field-strength,and rare-earth elements. Am Mineral 88(2–3):330–337. https://doi.org/10.2138/am-2003-2-310
White JC, Parker DF, Ren M (2009) The origin of trachyte and pantellerite from Pantelleria, Italy: insights from major element, trace element, and thermodynamic modelling. Journal of Volcanology and GeothermalResearch 179(1–2):33–55. https://doi.org/10.1016/j.jvolgeores.2008.10.007
Whitwort MP (1992) Petrogenetic implications of garnets associated with lithium pegmatites from SE Ireland. Mineral Mag 56:75–83
Zhu Y-F, Zeng Y, Gu L (2006) Geochemistry of the rare metal-bearing pegmatite no. 3 vein and related granites in the Keketuohai region, Altay Mountains, northwest China. J Asian Earth Sci 27:61–77